

## **Physical drivers and trends of the recent delayed withdrawal of the Southwest Monsoon over Mainland Indochina**

Kyaw Than Oo<sup>1,2,\*</sup>, Chen Haishan<sup>1,\*</sup>, Kazora Jonah<sup>1,3</sup>, Du Xinguan<sup>1</sup>

Key Laboratory of Meteorological Disaster, Ministry of Education/Joint International Research Laboratory of Climate and Environment Change/Collaborative Innovation Center on Forecast and Evaluation of Meteorological Disasters, Nanjing University of Information Science and Technology, Nanjing, 210044, People's Republic of China

## 2 Aviation Weather Services, Yangon, Myanmar

<sup>3</sup> Rwanda Meteorology Agency, Kigali, Rwanda

**\*Corresponding author:** [haishan@nuist.edu.cn](mailto:haishan@nuist.edu.cn), <https://orcid.org/0000-0002-2403-3187>,  
[kyawthanoo34@outlook.com](mailto:kyawthanoo34@outlook.com), <https://orcid.org/0000-0003-1727-3462>

## **Physical drivers and trends of the recent delayed withdrawal of the Southwest Monsoon over Mainland Indochina**

Kyaw Than Oo<sup>1, 2, \*</sup>, Chen Haishan<sup>1</sup>, Kazora Jonah<sup>1, 3</sup>, Du Xinguan<sup>1</sup>

<sup>15</sup> Key Laboratory of Meteorological Disaster, Ministry of Education/Joint International Research  
Laboratory of Climate and Environment Change/Collaborative Innovation Center on Forecast and  
Evaluation of Meteorological Disasters, Nanjing University of Information Science and Technology  
Nanjing, 210044, People's Republic of China

## 2 Aviation Weather Services, Yangon, Myanmar

<sup>3</sup> Rwanda Meteorology Agency, Kigali, Rwanda

\*Corresponding author: [kyawthanoe34@outlook.com](mailto:kyawthanoe34@outlook.com), <https://orcid.org/0000-0003-1727-3462>

### Key point

- Cumulative Change of Mainland Indochina Southwest Monsoon (MSwM) new definition index improves understanding of monsoon transitions.
- Anomalous trends of Subtropical Westerly Jet and Tropical Easterly Jet are linked to changes in wind patterns and monsoon timing.
- Anomalous Sea surface temperatures impact moisture transport during MSwM Retreat phases.

29 **Plain Language Summary**

30 The study investigates the delay withdrawal of the Mainland Indochina Southwest Monsoon (MSwM)  
31 by using spatial trend connections with meteorological and oceanic factors. The new Cumulative  
32 Change-Point Monsoon (CPM) definition index well described the definition of monsoon seasonal  
33 shifting. The results show that the subtropical westerly jet is getting stronger while the tropical easterly  
34 jet is getting weaker within these years. This influences the regional wind patterns and delays the  
35 monsoon withdrawal. The study highlights the critical role of ocean-atmosphere interactions and local  
36 atmospheric circulation in influencing the summer monsoon. Specifically, warmer sea surface  
37 temperatures in the Indian Ocean enhance moisture transport through strengthened southwesterly  
38 winds, while atmospheric pressure gradients drive moisture convergence over the region. These  
39 processes contribute to prolonged monsoon seasons, increasing the risk of floods and disrupting  
40 agricultural schedules, which significantly impact water management and farming in Mainland  
41 Indochina.

42 **Abstract**

43 The study investigates the key factors that cause the Mainland Indochina Southwest Monsoon (MSwM)  
44 to delay withdrawal, utilizing a spatial trend correlation between the monsoon index and various  
45 meteorological and oceanic variables such as sea surface temperature (SST), zonal winds, and moisture  
46 transport. A significant strengthening trend in the Subtropical Westerly jet (SWJ) and a weakening  
47 Tropical Easterly jet (TEJ) not only impacts regional wind patterns but also delays the monsoon  
48 departure. The anomalous South China Sea and the equatorial Indo-Pacific Ocean surface temperature  
49 (SSTA) further contribute to these delayed withdrawals, and there is a significant correlation between  
50 the MSwM withdrawal index and SSTA, moisture transport, and essential atmospheric factors. The  
51 results clarify MSwM dynamics, offering significant insights for future climate research associated  
52 with MSwM. The study also suggests that the variability of ocean-atmosphere interactions and local  
53 atmospheric circulation patterns is critical for understanding monsoon variability, which has a potential  
54 impact on climate predictions, water resource management, and agriculture practices over Mainland  
55 Indochina.

56 **Keywords:** Mainland Indochina, Monsoon Withdrawal, MSwM, SWJ, TEJ, ENSO

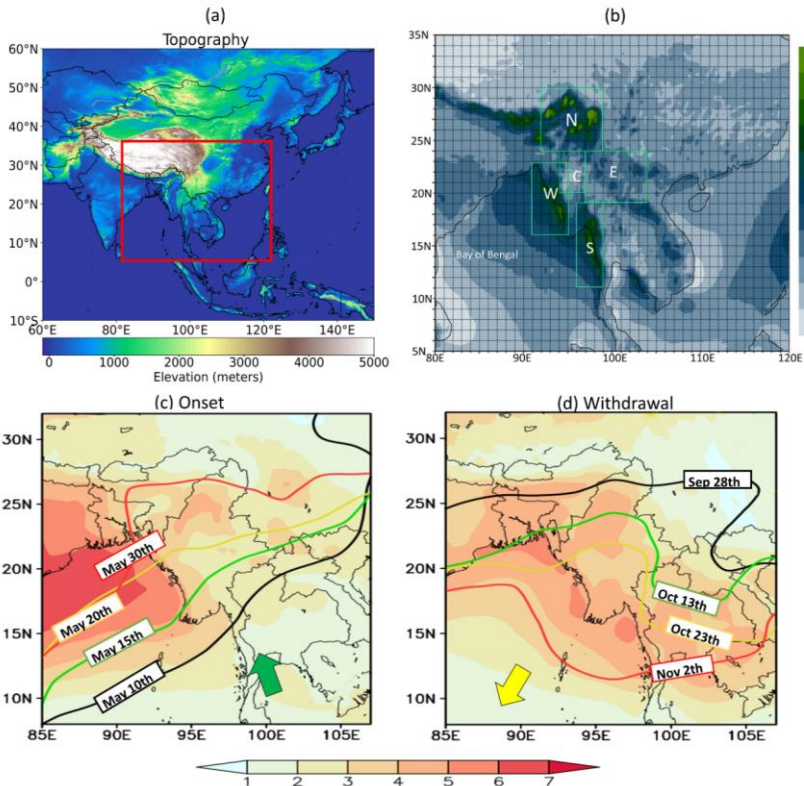
57 **1 Introduction**

58 In tropical Asia, the summer monsoon system is one of the most significant meteorological  
59 phenomena in the Northern Hemisphere. This monsoon onset and withdrawal are the most notable  
60 intraseasonal variable in monsoon systems. The beginning of the summer rainy season, extensive

61 convection, and a rapid change in atmospheric circulation characterize this period (Aung et al., 2017;  
62 Bordoni & Schneider, 2008; Salinger et al., 2014). Based on previous science literature of the Asia-  
63 Pacific monsoon classification, there are three primary types of summer monsoons, East Asian  
64 (EASM), Indian (ISM), and Western North Pacific (WNPSM) monsoons (B. Wang & Ho,  
65 2002), (Supplementary Fig S-1). The eastern bay of Bengal (EBOB), as known as the mainland-  
66 Indochina region (MIC) study area (Fig. 1Fig. 1a) is situated in a transitional zone between the (ISM)  
67 (India Summer Monsoon) and the WNPSM (Western North Pacific Summer Monsoon) systems (Op-  
68 & Jonah, 2024). The monsoon indices had been developed to study the transition and boundary  
69 between the Indian Summer Monsoon (ISM) and East Asian Summer Monsoon (EASM) (Cao et al.,  
70 2012), characterize monsoon onset and withdrawal using rainfall-based metrics (Bombardi et al., 2019;  
71 S. Zhang et al., 2024), and define these phases through circulation-based approaches (L. Chen et al.,  
72 2023; Hu et al., 2022). The MIC also features complex terrain, with high mountain ranges and long  
73 costal area. Simply, the MIC dominates a unique position between the southern areas of East and  
74 Middle East Asia, where this monsoon system over MIC exhibiting transitional characteristics between  
75 the two monsoon systems (Y. Zhang et al., 2002a). Consequently, significant variation in agricultural  
76 planting and ploughing times occur over MIC affected by the monsoon rainfall (Fig. 1Fig. 1b),  
77 depending upon the early or late monsoon onset or withdrawal.

Formatted: Font color: Blue

Formatted: Font color: Blue



78

79 Fig. 1 (a) Topography (m) of the study area, including mainland Indochina. (b) Daily rainfall (mm) during the MSwM season. (c) 80 Climatological onset and (d) withdrawal dates of MSwM with standard deviation values (shaded, days). This figure was created with 81 Python 3.10 (Matplotlib 3.5.2 [<https://matplotlib.org/>]), Cartopy 0.20.0 [<https://pypi.org/project/Cartopy/>]).

82 A range of onset and withdrawal indices has been established, based on rapid changes in extensive  
 83 atmospheric structures. Especially, the most commonly used atmospheric variables for defining onset  
 84 and withdrawal indices include rainfall (Ajayamohan et al., 2009; Colbert et al., 2015; Htway &  
 85 Matsumoto, 2011; Vijaya Kumari et al., 2018), and reversable component wind (CY Li, 1999; Li et  
 86 al., 2010; Webster & Yang, 1992). In addition to precipitation and circulation, the thermal and moisture  
 87 characteristics of the atmosphere also serve as an important indicator for describing the progression of  
 88 the monsoon season (Song et al., 2025; H. Zhang et al., 2012). The summer monsoon typically onset  
 89 to MIC between mid-May and early June, with slight variations in indices and statistics (Mao & Wu,  
 90 2007; Oo, 2023a; Ren et al., 2022; B. Wang & Ho, 2002). The MSwM withdrawal displayed significant  
 91 interannual variability, with a extent of one to two weeks may vary among the earliest and latest  
 92 withdrawals based on climatological data (Evan & Camargo, 2011; Oo, 2023a). In addition to ENSO,  
 93 recent studies have demonstrated that mid-high latitude systems also have significant impacts on

Formatted: Font color: Blue

94 [ENSO, East Asian monsoon onset and withdrawal, which should also be briefly reviewed](#) (Hu et al.,  
95 2020, 2025)

96 The global wind circulation and the El Niño Southern Oscillation (ENSO) have been widely  
97 studied for their influence on the interannual variability of monsoon onset (Roxy et al., 2014; R. Wu,  
98 2017), the formation of South Asia's subtropical high (Q Guo, 1988; B. Wang et al., 2008; Y. Zhang  
99 et al., 2002b), and fluctuations in local sea surface temperature (SST) (Salinger et al., 2014; Xu et al.,  
100 2023). Based on these long-term physical atmospheric variables data, this study seeks to examine the  
101 factors contributing to the delay withdrawal of the MSwM, with superior weight on ocean-atmosphere  
102 interactions and zonal wind dynamics, which have been insufficiently explored in this area, since  
103 monsoon rains are crucial for agriculture and fill up water supplies (Win Zin & Rutten, 2017; Zin Mie  
104 Mie Sein et al., 2015). In this study, we present the variability of withdrawal dates over interannual  
105 scale. Due to the significant up trending of local withdrawal date of MSwM, derived from the  
106 combination of reversal of winds circulation (Ramage, 1971) and vertical moisture flux transport  
107 changes (Fasullo & Webster, 2003). We investigate the mechanism driver of these delay withdrawal  
108 and potential driver of continues untimely rainfall after MSwM withdrawal.

## 109 2 Data and Method

110 The study utilizes data from five sources:

111 1. **Department of Meteorology and Hydrology, Myanmar (DMH):** Daily observed rainfall, sea  
112 level pressure, and annual onset and withdrawal dates for significant regions were collected from  
113 DMH, which operates 79 meteorological stations nationwide. This data help assess validate of  
114 reanalysis datasets.

115 2. **NCEP/NCAR Reanalysis:** This dataset provides zonal (u) and meridional (v) wind components,  
116 specific humidity (q), geopotential height (z), and vertical velocity (w) at atmospheric isobaric  
117 levels in the troposphere for wind analysis (Kanamitsu et al., 2002).

118 3. **European Centre for Medium-Range Weather Forecasts - ECMWF:** ERA5 offers reanalysis  
119 data with a 0.25° geographical resolution for global climate analysis, including sea level pressure  
120 (SLP), moisture flux convergence (MFC), and outgoing longwave radiation (OLR) for the period  
121 from 1991 to 2020 (Hersbach et al., 2020).

122 4. **Unified Gauge-Based Analysis of Global Daily Precipitation (CPC):** This dataset provides  
123 rainfall data (M. Chen et al., 2008; Jiao et al., 2021).

124 5. **Hadley Centre:** Hadley Centre Sea Surface Temperature dataset (HadISST) (Selman & Misra,  
125 2014).

126 **2.1.1 Definition of Monsoon onset and withdrawal by CPM index**

127 The MSwM region is defined by coordinates 10°N–30°N and 85°E–110°E (Fig. 1; see Appendix  
128 for additional details). We examine seasonal fluctuations in the moisture budget and extensive  
129 atmospheric circulation, as established by:

130 *Equation 1*

$$131 \quad MFC = - \int_{Surface}^{300hPa} \nabla_p \cdot (Uq) \frac{dp}{g} = P - E + \frac{\partial W}{\partial t}$$

132 This equation was developed from a prior study on the variability of the Asian Monsoon (Walker et  
133 al., 2015). In this context, Moisture Flux Convergence (MFC) is a vital quantity that delineates the  
134 equilibrium of moisture in the atmosphere. The initial segment of the equation encapsulates the  
135 dynamic component, represented by the divergence of moisture flow " $(Uq) \cdot \nabla p$ " denotes the  
136 movement and accumulation of moisture resulting from wind patterns. This dynamic element is  
137 essential for comprehending how atmospheric circulation patterns affect moisture availability. The  
138 second component, " $P - E + \partial W / \partial t$ " signifies the thermodynamic equilibrium of moisture inside the  
139 system. **P** represents precipitation, **E** signifies evaporation, and  $\partial W / \partial t$  reflects temporal variations in  
140 water storage. This relationship illustrates how thermodynamic mechanisms regulate the moisture  
141 budget and influence the overall climate dynamics of the monsoon zone.

142 By integrating dynamic and thermodynamic aspects, the cumulative change of the MSwM  
143 (CPM) index provides a strong framework for analyzing the behavior of the monsoon circulation over  
144 time. Building upon the MFC, we define the Cumulative Change of the MSwM (CPM) index of onset  
145 and withdrawal as follows:

146 *Equation 2*

$$147 \quad MSwM (CPM) = \frac{1}{5} * (D(U_1 - U_2) + D(P_1 - P_2) + D(MFC) + D(TP_{net}) + D(OLR))$$

148 These five diagnostic variables were used to characterize the onset and withdrawal of the monsoon  
149 over the transitional Mainland Indochina (MIC) region, outgoing longwave radiation (OLR), vertically  
150 integrated moisture flux convergence (MFC), net precipitation (TpNet), meridional shear in zonal  
151 winds (U1–U2), and pressure gradient (P1–P2). These variables are physically consistent with the  
152 governing moisture budget equation. We determine the normalized values for each factor annually for  
153 statistical investigation. The cumulative value change from positive to negative, or vice versa, is  
154 verified for further statistical calculations. "D" in Equation (2) expresses the date when the state shifts  
155 of positive or negative (+ to - or - to +) values and typically represents the change or difference in the  
156 standardize values of each variable in a year.

157     Thus, changes in MFC directly link large-scale circulation dynamics with rainfall variability,  
158     while TpNet (P-E) and OLR confirm convective activity and cloud cover. In this equation, D (U1-  
159     U2) and D(P1 - P2) represent the differences in zonal winds and pressure between the southern and  
160     northern regions of the Mainland Indochina (MIC). Specifically, the southern region (90°–100°E, 10°–  
161     15°N) reflects the influence of the broad Indochina Peninsula, where the southwest monsoon winds  
162     are most active, while the northern region (95°–100°E, 25°–30°N) captures the terrain-influenced  
163     pressure dynamics near the eastern Tibetan Plateau (Fig. 1Fig. 1a) and the southwest monsoon wind  
164     withdrawal pattern (Fig. 1Fig. 1d), we take pressure readings that are different from longitude ranges  
165     as two distinct regions. The meridional shear in the 850-hPa zonal winds and the pressure gradient  
166     between northern and southern regions which is driving monsoon flows, the key indicators of monsoon  
167     circulation, are averaged across two distinct regions: the southern MIC (90E-100E, 10N-15N), referred  
168     to as (U1,P1), and the northern MIC (95E-100E, 25N-30N), designated as (U2,P2). This approach  
169     follows the Gill-type tropical circulation response (Gill, 1980), where deep convection excites  
170     westward-propagating Rossby wave responses that enhance southwesterlies to the west of the  
171     convention center, and the South China Sea–Bay of Bengal circulation system provides a dynamical  
172     link between ISM and WNPSM (B. Wang et al., 2009; X. Wang & Zhou, 2024). Consequently, the  
173     five indices together capture the coupled thermodynamic and dynamic drivers of monsoon evolution  
174     in this transitional region. The term D(MFC) captures the cumulative changes in moisture transport  
175     and convergence, essential for monsoon rainfall, while D(TPnet) represents net precipitation changes,  
176     indicating monsoon withdrawal as well as onset by rainfall and D(OLR) the changes in outgoing  
177     longwave radiation, closely linked to convective activity and cloud cover to confirm monsoon rainfall,  
178     respectively. We calculate the mean change date of the standardized positive/negative value of the  
179     outgoing longwave radiation (OLR), the vertically integrated moisture budget transition (MFC), the  
180     net precipitation (TpNet), the meridional shear wind (U1-U2) (U-wind), and the pressure differential  
181     (P1-P2) (dP). The first day of three consecutive positive or negative days is taken into consideration  
182     when determining the change date. Next, we obtained each variable's change point dates for every year.  
183     Lastly, the climatology data for every term date was acquired (Supplementary Table S1). We used  
184     these findings to compute the MSwM Change Point Index, which is the arithmetic mean onset dates,  
185     withdrawal dates, and season length (Supplementary Table S4). A student's t-test is used to calculate  
186     the correlation coefficients of these findings at the 95% level of significance. This rounded approach  
187     allows for a comprehensive assessment of the interrelationships among these parameters, simplifying  
188     the identification of key onset (Fig. 1Fig. 1c) and withdrawal (Fig. 1Fig. 1d). Moreover, common  
189     statistical methods such as correlation (Krugman et al., 2018), regression (Ma, 2019), random forest  
190     (Breiman, 2001), box and whisker (Schmidhammer, 2000) are also applied in the study at necessary  
191     parts.

Formatted: Font color: Blue

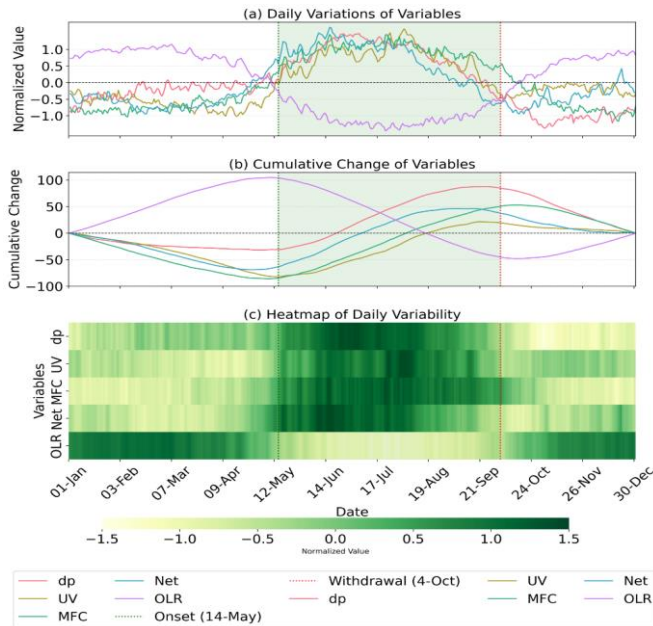
192 The Random Forest technique, a widely used ensemble machine-learning method, was utilized to  
193 find the relative relevance of variables controlling monsoon withdrawal and rainfall. It generates  
194 several decision trees during training by sampling subsets of data and features, hence mitigating  
195 overfitting and enhancing generalization (Breiman, 2001). Our study incorporated input variables  
196 comprising atmospheric and hydrological factors, including Outgoing Longwave Radiation (OLR),  
197 Net Precipitation (Net), Moisture Flux Convergence (MFC), Zonal Wind Shear (U), and Pressure  
198 Differential (dP). Each tree generated a prediction, and the final output was ascertained by averaging  
199 (for regression tasks) or by majority voting (for classification tasks). Box and whisker plots were  
200 employed to graphically encapsulate the distributions of essential variables across various phases of  
201 the monsoon season (Schmidhammer, 2000). It is good to examine the day-of-year distributions for  
202 monsoon withdrawal timing based on many factors, including dP, U, MFC, Net Precipitation, and  
203 OLR. This analysis clearly exhibited variability and key tendencies in the data, highlighting the  
204 contribution of specific variables to withdrawal patterns. For example, zonal wind shear (U) exhibits  
205 narrower variability, indicating a more consistent relationship with withdrawal timing compared to  
206 other factors.

207 

### 3 Results and Discussion

208 

#### 3.1 Climatology Outlook



209

210 Fig. 2 Daily and cumulative variations of monsoon parameters with their seasonal progression. (a) Daily variations of normalized  
 211 parameters: pressure gradient (dp; red), wind shear (UV; yellow), moisture flux convergence (MFC; green), net precipitation (Net;  
 212 blue), and outgoing longwave radiation (OLR; purple). (b) Cumulative changes of the same parameters with identical color coding.  
 213 (c) Color strip timeseries showing the daily variability of all parameters throughout the year. Vertical dotted lines indicate monsoon  
 214 onset (green; 14-May) and withdrawal (red; 4-Oct), with light green shading highlighting the monsoon active period in (Fig a nd b). All  
 215 parameters are normalized and calculated according to Eqs. (1) and (2). This figure was created using Python 3.10 with Matplotlib  
 216 3.5.2 (<https://matplotlib.org/>) and Seaborn.

217 Fig. 2 explained how the MSwM (CPM) index is constructed by combining both thermodynamic  
 218 and dynamic climatology daily contribution (Fig. 2.a) and their cumulative change (Fig. 2.b) of same  
 219 variables. Cumulative change curves (CMFC, Cdp, Cwind) help track the transitions in atmospheric  
 220 conditions that define the onset and withdrawal of the monsoon. The simultaneous positive and  
 221 negative shifts in MFC, OLR, pressure differentials, and wind shear facilitate the identification and  
 222 calculation of monsoon onset and withdrawal. Both figures underscore the significance of cumulative  
 223 effects in the MSwM index, where prolonged alterations over several days in moisture flux, wind shear,  
 224 and pressure differentials signify critical transitions in the monsoon cycle, thereby illustrating the  
 225 seasonal progression of the monsoon in contrast to mere daily variations. The Color strip timeseries  
 226 (Fig. 2.c) support more clarity transaction of monsoon season by same variables values. The  
 227 climatology dates for each year are shown in Table S-1 and S-2 of the supplemental material.

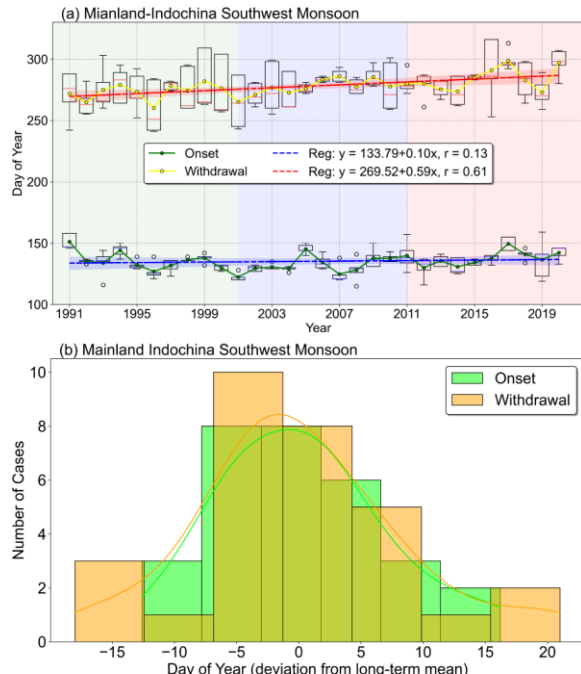
228        However, the small asynchrony among variables in Fig. 2 arises because each diagnostic reflects  
229        different aspects of the monsoon system with distinct adjustment timescales: dynamical fields (wind  
230        shear, pressure gradient) respond rapidly to convective heating through Gill-type circulation, while  
231        thermodynamic fields (MFC, TpNet, OLR) involve moisture storage and cloud-radiation feedbacks  
232        that introduce short lags (Gill, 1980; B. Wang et al., 2009). The CPM index minimizes this effect by  
233        averaging across all five variables, so that the central onset and withdrawal dates are robust, while the  
234        spread provides an objective measure of uncertainty.

235        Some studies have indicated that the monsoon onset over the Bay of Bengal is significantly  
236        correlated with that over the South China Sea and India (Xing et al., 2016). The India Monsoon Index  
237        (IMI), the Webster and Yang monsoon index for Asia (WYI), the West North Pacific monsoon index  
238        (WNPMI), and are some of the well-known monsoon indicators for the South Asian region (Goswami  
239        et al., 1999; B. Wang et al., 2001, 2004; Webster & Yang, 1992). However, seasonal wind variation  
240        and uniform rainfall can also be used to designate MSwM zones as sub-regions (Oo, 2022a, 2023b).  
241        In terms of annual variability, MSwM and other South Asian monsoon indicators show a comparable  
242        time-series pattern and a positive moderate connection (Supplementary Fig S-6).

Formatted: Font color: Blue

Formatted: Font color: Blue

Formatted: Font color: Blue



243

244 Fig. 3 (a) Interannual variability of MSwM onset (green line) and withdrawal (yellow line) dates, with trends.  
 245 (b) Frequency distribution of deviations from mean onset and withdrawal dates, with implications for Indochina agriculture.  
 246 This figure was created with Python 3.10 (Matplotlib 3.5.2 (<https://matplotlib.org/>)).

247 Examining the distribution patterns of the onset and withdrawal dates of the MSwM across  
 248 MIC is interesting, despite the MSwM index reflecting changes in the whole MIC rather than a specific  
 249 region within its domain. In this study, we only consider interannual variability over southern region  
 250 (95E-100E, 10N-15N) ("S" area in Fig. 1Fig. 1.b) where is the first onset point (during onset) and last  
 251 withdrawal point (during withdrawal) in north-south-north shifting of monsoon characteristic due to  
 252 its role in the migration of the Intertropical Convergence Zone (ITCZ), which shifts northward during  
 253 boreal summer, initiating intense convective activity and precipitation. At this latitude, the strong land-  
 254 ocean thermal contrast generates a pressure gradient, drawing moist southwesterly winds from the  
 255 Indian Ocean that converge and bring rainfall (Goswami & Xavier, 2005). This region aligns with the  
 256 early onset of monsoon rainbands and moisture convergence observed in climatological data, as well  
 257 as the geographical position of southern Myanmar, India and Sri Lanka, which are the first landmasses  
 258 to experience the advancing monsoon (K Lau, 2000). Fig. 3.a shows interannual variation of onset and  
 259 withdrawal dates with their trend including whisker statistical box. It indicates the timing of onset and  
 260 withdrawal phases, which are vital for understanding how the regional monsoon system is developing.

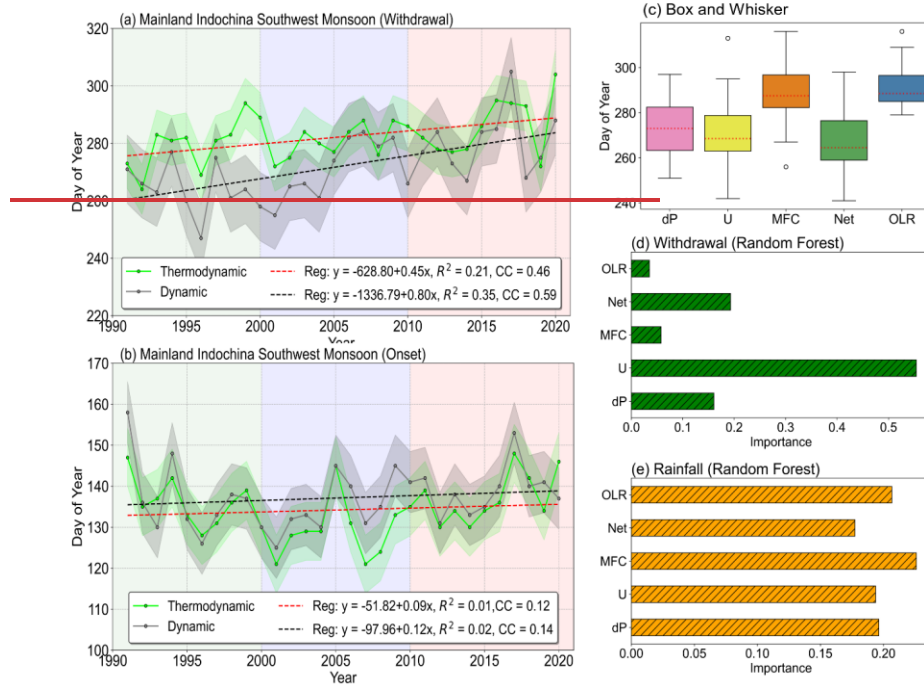
Formatted: Font color: Blue

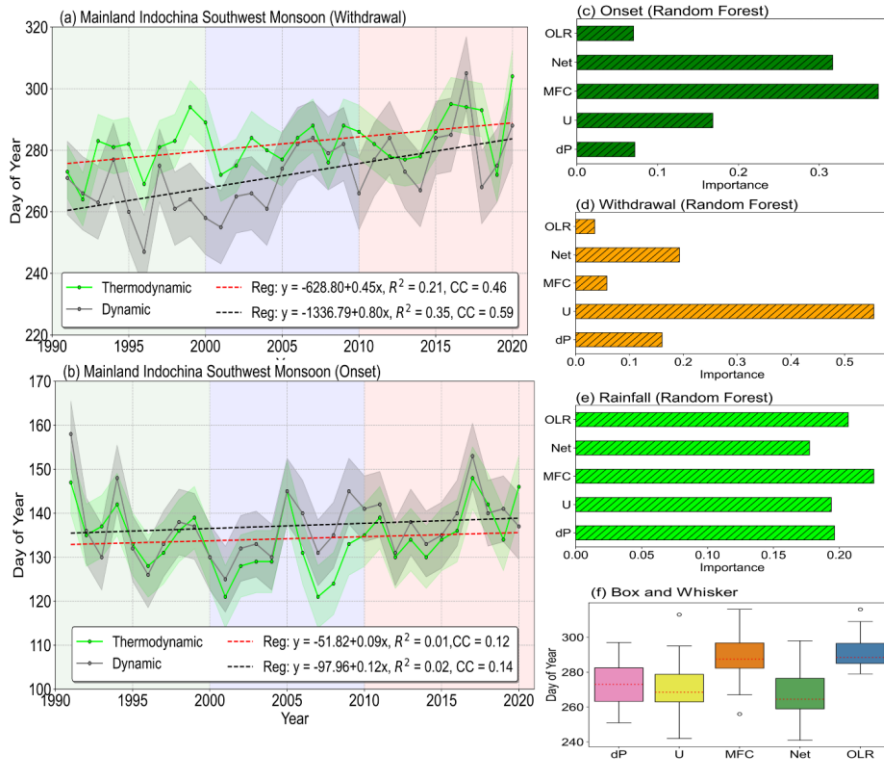
261 Over the MIC, early or delayed onset and withdrawal of the monsoon can dramatically affect the  
262 seasonal rainfall patterns, which may lead to regional crop production and society plans. The trend  
263 lines in both phases suggest possible long-term shifts in monsoon behavior (Fig. 3.a), may be influence  
264 of the broader climatic drivers such as variability of ENSO or Indian Ocean dipole (IOD) (Ding et al.,  
265 2011a; B. Wang & Ho, 2002). While ENSO/IOD influence monsoon dynamic circulation, their direct  
266 impact on MSwM onset timing is secondary to regional thermodynamics (Oo, 2021, 2022b; Oo et al.,  
267 2025; Oo & Jonah, 2024). The timeseriestime-series of dynamic and thermodynamic trend displayed  
268 that withdrawal dates are significantly greater variation than onset dates within five variables of CPM  
269 index for each year especially in dynamic boundary (Fig. 4). The frequency distribution of deviations  
270 from the mean onset and withdrawal dates (Fig. 3.b), which explained that onset and withdrawal date  
271 may early or delay generally one to two weeks (5 to 7 days as usual in general). The longest delay  
272 (early) withdrawal phases occurred with 20 days (15 days) during this 30-year study period 1991-2020.  
273 The onset phases are generally characterized by a rapid shift in moisture flux and dynamic  
274 transformations over MIC, whereas the withdrawal phases occurs more gradually and may be affected  
275 by extensive atmospheric patterns (Seager et al., 2010), including modifications in subtropical jets,  
276 mid-latitude disturbances, and tropical easterly waves, which can introduce variability in the timing of  
277 the retreat (Hu et al., 2019).

**Formatted:** Font: Not Italic, Complex Script Font: Not  
Italic

**Formatted:** Font: Not Italic, Complex Script Font: Not  
Italic

**Formatted:** Font: Not Italic, Complex Script Font: Not  
Italic





279  
280 Fig. 4 Interannual variation of thermodynamic and dynamic factors during (a) onset and (b) withdrawal phases of MSwM, with trends,  
281 highlighting the impact on mainland Indochina (c) the box whisker plot of five physical parameters to determine the MSwM onset and  
282 withdrawal (Oo et al. 2023). And their sensitivity tests by random forest method (d) for CPM index onset, (d) for CPM index withdrawal  
283 and (e) for monsoon regional rainfall. (f) The boxplots whisker plot of five physical parameters to determine the MSwM onset and  
284 withdrawal (Oo et al. 2023). This figure was created with Python 3.10 (Matplotlib 3.5.2 [<https://matplotlib.org/>]).

285 The interannual variation trends of the onset and withdrawal dates of MSwM from 1991 to 2020, have  
286 a clear divergence in behavior between the two phases while studied split into dynamic and  
287 thermodynamic according to CPM index (Fig. 4). The onset of the MSwM shows slight changes over  
288 time, with weak regression slopes of 0.09 and 0.12 days per year for the thermodynamic and dynamic  
289 components respectively under weak statistically significant (Fig. 4.b). However, the withdrawal phase  
290 exhibits a much more marked positive trend, especially the dynamic component has an even steeper  
291 slope of 0.80 days per year, while thermodynamic component for withdrawal shows a regression slope  
292 of 0.45 days per year with 95% statistically significant respectively (Fig. 4.a). This indicates that  
293 dynamic factors, such as changes in large scale wind patterns, are playing a more significant role in  
294 driving the delayed monsoon withdrawal.

295 The box plot (Fig. 4.e) reveals that MFC and OLR correspond to delay withdrawal dates,  
296 indicating that delayed MFC may play key roles in postponing the withdrawal. The result is generally  
297 correct due to the rainfall days remaining due to regional local convective activities and tropical  
298 cyclone effect during the post monsoon season (Akter & Tsuboki, 2014; Fosu & Wang, 2015; Oo et  
299 al., 2024). When we go dive into this, Fig. 4.e displays that monsoon rainfall variability is impacted  
300 by U, dP, MFC, and OLR, though their standing is more evenly spread, the random forest results  
301 highlight U (850 hPa zonal wind) as the most critical factor driving the withdrawal, followed by dP  
302 (Fig. 4.d). The strong influence of U suggests that zonal wind shifts, possibly linked to tropical  
303 disturbances such easterly wave from south China sea, upper jet stream anomaly, local tropical  
304 cyclones, could further affect the timing of withdrawal. This indicates that rainfall events are still  
305 remain usual even after the monsoon winds was withdrawal from the study region (Chou et al., 2009).  
306 To reach this conclusion, we will go further into the next section. The interannual variations of the  
307 Mainland Indochina Southwest Monsoon (MSwM) onset and withdrawal dates from 1991 to 2020  
308 reveal a clear divergence in behavior between the two phases when analyzed through thermodynamic  
309 and dynamic components using the CPM index (Fig. 4). The onset phase shows minimal long-term  
310 change, with weak regression slopes of +0.09 days/year for the thermodynamic component and +0.12  
311 days/year for the dynamic component, both statistically insignificant (Fig. 4.b). In contrast, the  
312 withdrawal phase exhibits a significant delay, especially in the dynamic processes, with a regression  
313 slope of +0.80 days/year and a moderate correlation ( $R^2 = 0.35$ , CC = 0.59). The thermodynamic  
314 component also shows a positive trend, albeit weaker, at +0.45 days/year ( $R^2 = 0.21$ , CC = 0.46),  
315 indicating that dynamic atmospheric factors, such as upper-level wind changes, are increasingly  
316 contributing to the delayed monsoon withdrawal (Fig. 4.a).

Formatted: Font color: Blue

Formatted: Font color: Blue

Formatted: Font color: Blue

317 The random forest analysis further supports these findings. For onset prediction, the Net heat  
318 flux (Net) and Moisture Flux Convergence (MFC) are the most important factors, reflecting the  
319 dominant role of thermodynamic processes (Fig. 4.c). For withdrawal prediction, however, the 850-  
320 hPa zonal wind (U) emerges as the most critical driver, followed by pressure gradient (dP), with MFC  
321 playing a secondary role (Fig. 4.d). Regarding seasonal rainfall, all five parameters (U, dP, MFC, Net,  
322 OLR) contribute relatively evenly (Fig. 4.e), highlighting the coupled influence of both dynamic and  
323 thermodynamic factors on rainfall variability.

Formatted: Font color: Blue

Formatted: Font color: Blue

Formatted: Font color: Blue

324 The box-whisker plot (Fig. 4.f) shows that MFC and OLR tend to correspond with delayed  
325 withdrawal dates, suggesting that lingering moisture convergence and persistent convective activity  
326 can postpone the withdrawal phase. This aligns with previous findings that regional convective  
327 systems and late-season tropical cyclones (Akter & Tsuboki, 2014; Fosu & Wang, 2015; Oo et al.,  
328 2024) can sustain rainfall events even after large-scale monsoon winds weaken (Chou et al., 2009).

Formatted: Font color: Blue

329 These results collectively point to a dynamic-thermodynamic asymmetry: while monsoon onset is  
330 controlled primarily by energy build-up and moisture availability, the withdrawal is increasingly  
331 modulated by dynamic atmospheric circulation anomalies, such as upper-level wind changes and  
332 tropical disturbances from the South China Sea (X. Wang & Zhou, 2024).

333 The analysis suggests that the two phases of monsoon are influenced by distinct mechanisms  
334 with weak interdependence. The onset phase remains stable over the study period, primarily driven by  
335 thermodynamic factors, while the withdrawal phase shows a significant delay due to dynamic factors  
336 (Fig. 4). This decoupling might be explained by different large-scale climate processes governing the  
337 two phases: onset is mainly linked to pre-monsoon land-sea thermal contrasts and moisture build-up,  
338 whereas withdrawal is more sensitive to post-monsoon circulation shifts, tropical cyclone activity, and  
339 upper-level wind anomalies. However, this finding also highlights the need for further research into  
340 potential indirect links, such as how early or late onsets may influence intra-seasonal rainfall breaks,  
341 which in turn could modulate withdrawal characteristics.

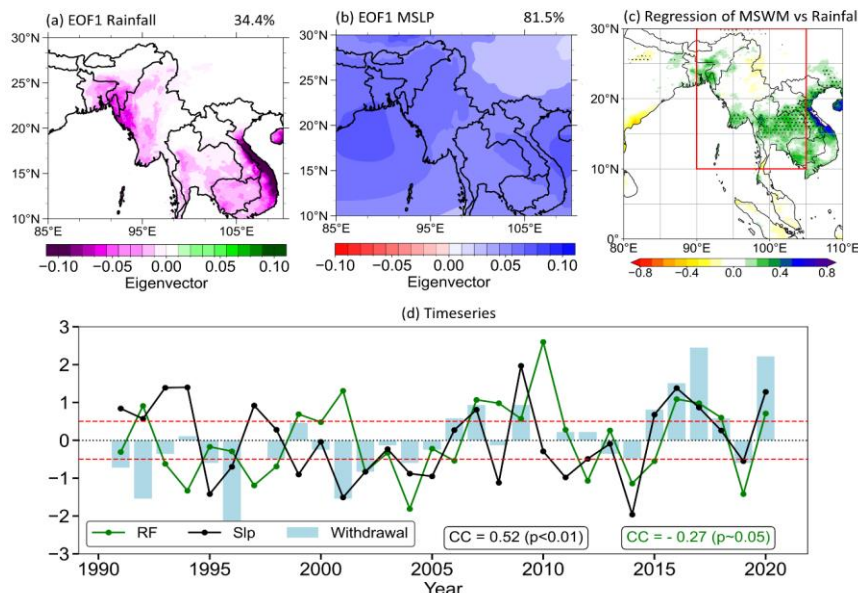
Formatted: Font color: Blue

### 342 3.2 Variation of MSwM withdrawal dates and Rainfall in October

343 The first Empirical Orthogonal Function (EOF) modes of October rainfall and mean sea level  
344 pressure over the study area, and their normalized principal components (PCs) expressed in Fig. 5Fig.  
345 5. The first EOF for rainfall, explaining 34.4% of the variance (Fig. 5Fig. 5.a) and the first EOF for  
346 MSLP, explaining a larger 81.5% of variance, indicating its stronger influence on regional climate (Fig.  
347 5Fig. 5.b). Positive and negative eigenvectors suggest the impact of MSLP and rainfall distribution  
348 over withdrawal phases that reduction in rainfall and increasing in pressure. The regression between  
349 monsoon withdrawal dates by MSwM definition index (CPM) and regional rainfall explained positive  
350 relations (green areas in Fig. 5Fig. 5.c) suggest that the index can significantly reflect the October  
351 rainfall over the study area with 95% confidence. This show CPM index is significantly reflected to  
352 southern MIC ("S" area in Fig. 1Fig. 4.b), where is the last point of monsoon withdrawal, regional  
353 rainfall during withdrawal phases. Moreover, PCs time series of rainfall (RF), and SLP, from 1991 to  
354 2020 (Fig. 5Fig. 5.d), are comparing with monsoon withdrawal dates and the correlation between  
355 withdrawal dates and SLP shows 0.41, and between RF exhibited 0.24, with statistically confidence  
356 ( $p > 0.05$ ). However, the weak correlation between withdrawal timing and PCs RF suggests that while  
357 the timing of monsoon withdrawal affects the overall seasonal rainfall, it does not directly influence  
358 the spatial distribution of rainfall. This is because spatial distribution is primarily governed by local  
359 factors such as topography, moisture transport, and mesoscale atmospheric dynamics rather than the  
360 withdrawal timing alone. A late withdrawal may extend the period of rainfall over certain regions,  
361 increasing total rainfall. This dominant EOF modes capture the large-scale spatial variability of  
362 October rainfall and sea level pressure pattern, which is vital for understanding the dynamics of the

Formatted: Font color: Blue

363 transition from the warm wet southwest monsoon to the cold dry northeast monsoon season over MIC  
 364 (Hannachi, 2004; Oo, 2022c; X. Wu & Mao, 2018).



365  
 366 Fig. 5 First EOF modes of (a) rainfall and (b) Slp. (c) The regression values of withdrawal CPM indexd and regional october rainfall  
 367 with dotted area of 95% statistically confident by t-test. (d) The interannual vartaiton of normalized PCs of first two EOF and normalized  
 368 MSwM withdrawal dates with their correlation CC by respective color. The horizontal red dotted sperated the late ( $>0.5$ ) and early ( $<-0.5$ )  
 369 withdrawal years by their normalized anoamlies varues. This figure was created with Python 3.10 (Matplotlib 3.5.2  
 370 [<https://matplotlib.org/>], Cartopy 0.20.0 [<https://pypi.org/project/Cartopy/>]).

371 In addition, the SLP patterns are directly related to the atmospheric circulation that initiatives  
 372 rainfall and weather conditions over the region (Loikith et al., 2019). The shift in the SLP pattern could  
 373 indicate changes in the positioning of the low-level monsoon winds and subtropical high-pressure  
 374 systems, which bring the moisture-flux into mainland Indochina (Liu et al., 2021) (Fig S-5 in  
 375 supplementary ). The PCs associated with these modes provide a temporal perspective, indicating how  
 376 these dominant patterns advance over time. To perform composite analysis we collected eight delay  
 377 withdrawal years (2006, 2007, 2009, 2015, 2016, 2017, 2018 and 2020) and eight early withdrawal  
 378 years (1991, 1992, 1995, 1996, 2001, 2002, 2004 and 2019) by anomalies timeseries with PCs, we  
 379 collected positive(negative) 0.5 ( +/- renormalize 5-7 days) values years into late (early) withdrawal  
 380 years.

381 **3.3 Composite**

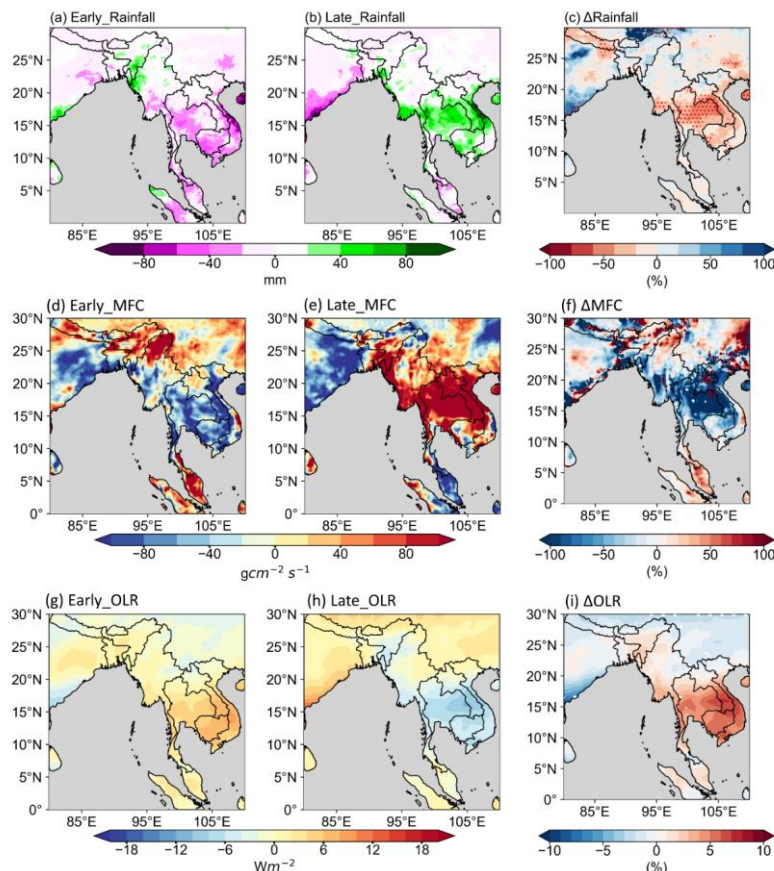
382 The composite anomalies analysis of three majors' variables what are used to define monsoon  
 383 onset and withdrawal are explained in [Fig. 6](#). The climatological values between early years (first  
 384 column) and late years (middle column), with their percentage difference (last column) over mainland  
 385 Indochina, were compared. The analysis indicates notable patterns in the distribution of monsoonal  
 386 rainfall, especially in southern MIC. The difference % map delineates areas where rainfall has either  
 387 diminished or increased, namely over southern MIC ([Fig. 6](#) and [Fig. 6.a](#) and [Fig. 6.b](#)). Their different percentages  
 388 also result significantly in the same region as shown in [Fig. 6](#) and [Fig. 6.c](#). This confirmed that the most  
 389 accurate classification skill of the MSwM CPM index over this southern MIC region as in ([Fig. 5](#) and [Fig. 5.c](#)).  
 390

**Formatted:** Font color: Blue

**Formatted:** Font color: Blue

**Formatted:** Font color: Blue

**Formatted:** Font color: Blue



391

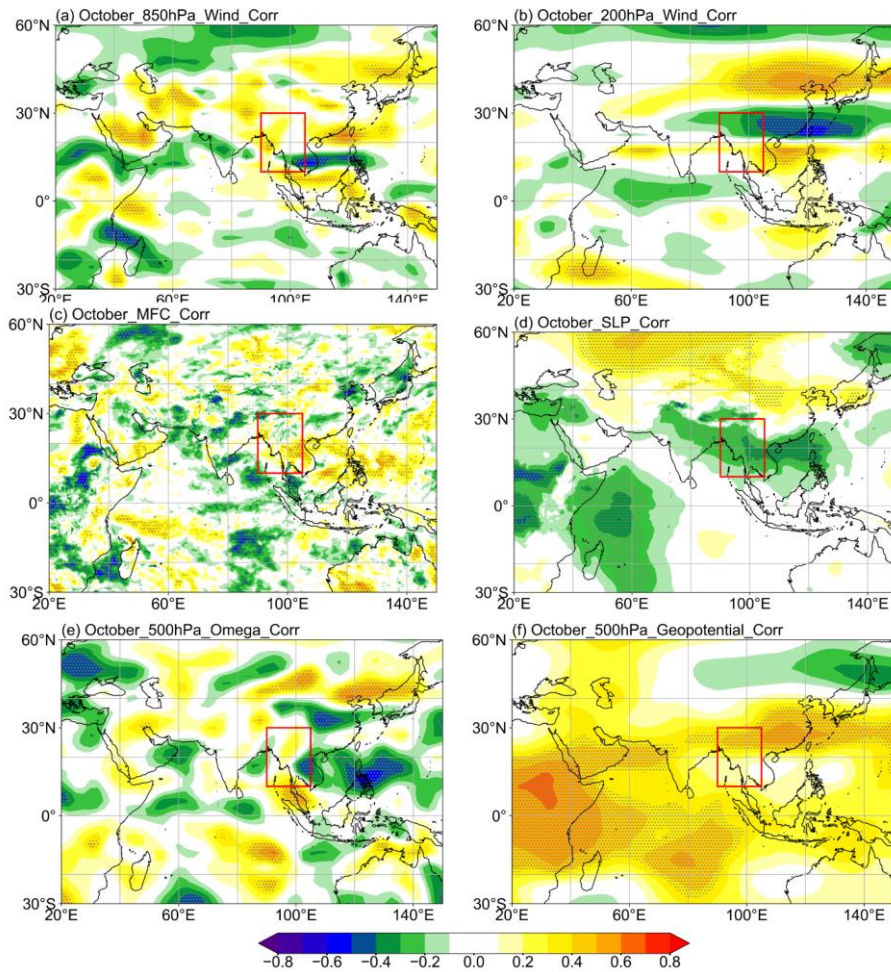
392 *Fig. 6 Climatological anomalies mean rainfall (mm), MFC ( $g/cm^2/s$ ) and mean OLR ( $Wm^{-2}$ ) for (a,d,g) early years, (b,e,h) late years,  
 393 and (c,f,i) the percentage difference, illustrating changing moisture dynamics over mainland Indochina. Red dotted show the area of*

394 95% statistically confident by *t*-test. This figure was created with Python 3.10 (Matplotlib 3.5.2 [<https://matplotlib.org/>]), Cartopy 0.20.0  
395 [<https://pypi.org/project/Cartopy/>]).

396 Changes in Moisture Flux Convergence (MFC) also impact rainfall patterns, with decreased  
397 MFC potentially reduction rainfall and increasing it, leading to wet conditions (Fig. 6 Fig. 6.c and d).  
398 The figure compares climatologically to mean MFC in low-lying areas over southern MIC show  
399 similar negative/ positive patterns is ~~validation~~ ~~validated~~ by their different values (Fig. 6 Fig. 6.f). Same  
400 patterns are also found for OLR of early and late withdrawal years over southern MIC. Thus, the  
401 MSwM CPM index is significantly reflected in this area.

Formatted: Font color: Blue

Formatted: Font color: Blue



402  
403 Fig. 7 Correlation between withdrawal date and October (a) 850 hPa wind, (b) 200 hPa wind, (c) MFC, (d) SLP, (e) 500 hPa Omega,  
404 and (f) 500 hPa geopotential, highlighting the drivers of monsoon withdrawal in mainland Indochina. Dotted shows the area of 90%

405 statistically confident by t-test. This figure was created with Python 3.10 (Matplotlib 3.5.2 (<https://matplotlib.org/>), Cartopy 0.20.0 (<https://pypi.org/project/Cartopy/>)).

407 The correlation between these various atmospheric variables, showing how relation of these  
408 variables with the delayed monsoon withdrawal (Fig. 7Fig. 7). The correlation between the withdrawal  
409 date and wind speed was calculated at each grid point, analyzing the withdrawal date against both the  
410 u-component and v-component speed. Statistical significance was determined using a student's t-test,  
411 with the dotted areas marking regions where the correlation is significant at the 90% confidence level.  
412 The correlations for 850 hPa wind speed (Fig. 7Fig. 7.a) expose strong negative relationships over  
413 MIC, indicating that weaker low-level winds contribute to the delay in withdrawal. This aligns with  
414 the positive-negative-positive trend pattern as in the Fig. 8Fig. 8.a and c, where negative correlations  
415 suggest a weakened low-level wind over MIC. In contrast, the 200 hPa wind correlation (Fig. 7Fig.  
416 7.b) shows a positive relationship, particularly over the northern regions, suggesting stronger upper-  
417 level winds during delayed monsoon retreat periods, which likely strengthens the subtropical westerly  
418 jet (SWJ) region and weakening in Tropical Easterly Jet region (TEJ). The SWJ, defined as a dominant  
419 westerly wind stream at approximately 200 hPa in mid-latitudes, and the TEJ, a tropical Easterly wind  
420 at similar altitudes. Similar patterns are also exhibited in trend plots Fig. 8Fig. 8. b and d. A delayed  
421 withdrawal sustains the thermal gradient between the Indian Ocean and the Asian continent,  
422 maintaining a strong meridional temperature gradient in the upper troposphere and thereby intensifying  
423 the SWJ. Simultaneously, the TEJ weakens due to reduced upper-tropospheric divergence and the  
424 diminishing impact of tropical heating as the monsoon season transitions.

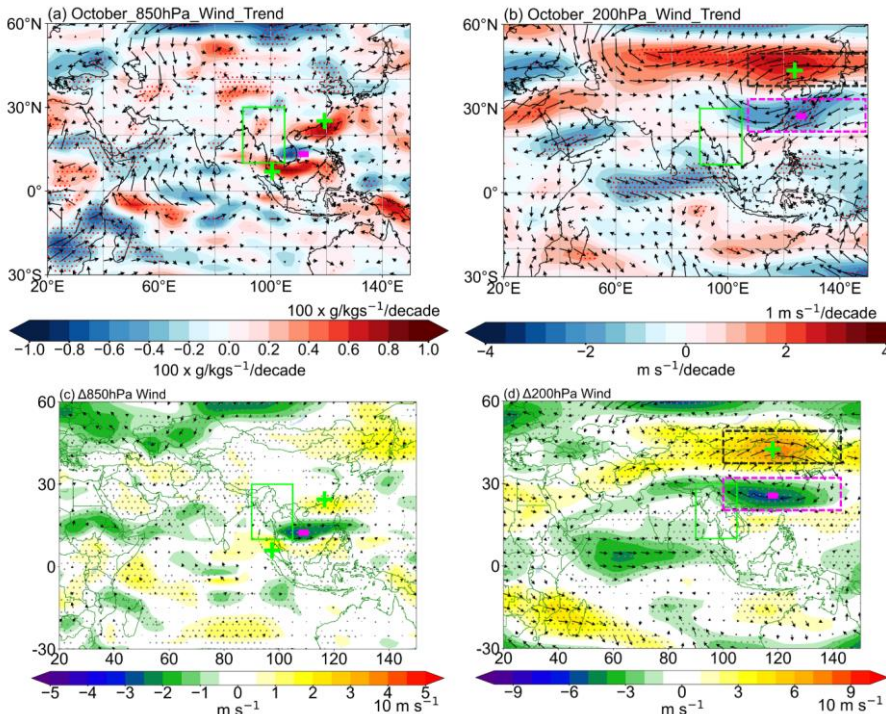
425 The correlation with Moisture Flux Convergence (MFC) (Fig. 7Fig. 7.c) also specifies a  
426 significant positive relationship in key study areas and positive trends also exhibited over same area  
427 (Fig. S-7 in supplementary). This positive trend suggests that delayed monsoon withdrawal is  
428 associated with stronger moisture convergence, trapping moisture likely to experience rainfall in  
429 southern MIC for a longer period and it's also association with previous composite analysis as in Fig.  
430 6Fig. 6. The Sea Level Pressure (SLP) correlation (Fig. 7Fig. 7.d) also shows a study area of negative  
431 correlation, which suggests that lower pressure systems dominate during delayed withdrawal,  
432 promoting cyclonic activities that extend the monsoon season and rainfall. Meanwhile, the positive  
433 correlations with 500 hPa Omega (Fig. 7Fig. 7.e) highlight the role of vertical motion over southern  
434 MIC, where positive Omega values (upward motion) correlate with a delayed withdrawal, can lead to  
435 cloud formation and rainfall if the conditions are right. Moreover, the 500 hPa geopotential positive  
436 correlations (Fig. 7Fig. 7.f) also show a weakened mid-tropospheric ridge over the subtropics with  
437 positive trend (Fig. S-7 in supplementary), leading to the late monsoon withdrawal as the atmospheric  
438 circulation shifts.

Formatted: Font color: Blue

439 The wind trends and anomalies highlight a significant alteration in both the lower (850 hPa)  
440 and upper (200 hPa) wind patterns (Fig. 8Fig. 8). The 850 hPa wind pattern (Fig. 8Fig. 8.a) indicates  
441 a weakening easterly flow over the South China Sea and southern MIC, and the 200 hPa wind trend  
442 (Fig. 8Fig. 8.b) indicates an intensification of the westerly flow linked to the SWJ, enhancing the  
443 upward motion and which may lead to anomaly lower-upper dynamic circulation patterns, and it may  
444 lead to delaying the timing of seasonal withdrawal of the monsoon. There is a noticeable positive-  
445 negative zonal wind anomaly pattern, especially at the 200 hPa level, in the difference in wind structure  
446 between late and early years (late years minus early years) at both altitudes, and this pattern changes  
447 significantly over time (Fig. 8Fig. 8.c and d). Delays in the MSwM withdrawals are directly affected  
448 by changes in jet stream dynamics, such as the strengthening of the SWJ and the weakening of the  
449 Tropical Easterly Jet (TEJ). The results of these additional investigations provided confirmation of this  
450 pattern of dynamic abnormality. Specifically, across the SWJ and TEJ regions, variations in wind  
451 intensity and direction are critical in affecting the delayed withdrawal trend, according to the CPM  
452 index analysis of these dynamic circulation patterns. Important regions where wind anomalies are  
453 strongly linked to delayed withdrawal are highlighted by the plus and minus signs in the Fig. 8. This  
454 emphasizes as they indicate critical areas where wind anomalies are closely associated with delayed  
455 withdrawal.

Formatted: Font color: Blue

Formatted: Font color: Blue



457  
458  
459  
460 Fig. 8 The spatial trend of (a) 850hPa horizontal moisture transport( $\text{g}/\text{kg}\text{s}^{-1}$ ) and 200hPa wind component (m/s). Percentage difference  
461 (late minus early) in horizontal wind patterns at (c) 850 hPa, and (d) 200 hPa between late and early years of MSwM withdrawal month  
462 October during 1991-2020. Red and grey dotted show the area of 95% statistically confident by t-test. This figure was created with  
463 Python 3.10 (Matplotlib 3.5.2 [<https://matplotlib.org/>]), Cartopy 0.20.0 [<https://pypi.org/project/Cartopy/>]).

456

457  
458  
459  
460

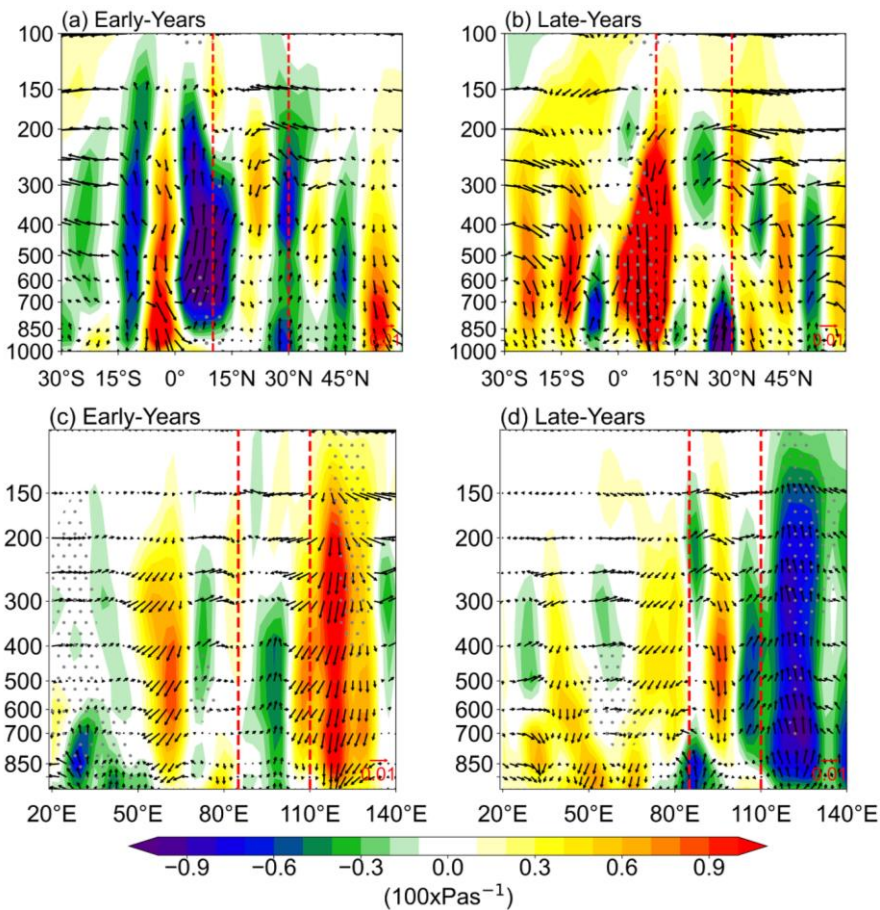
461  
462  
463  
464  
465  
466  
467  
468

The vertical structure of zonal wind, vertical motion, and moisture transport, comparing early and late years of the monsoon are exhibited in Fig. 9. The cross-section of vertical velocity over mainland Indochina, which is essential for understanding how wind circulation at different atmospheric layers contributes to vertical motion and convective processes (Kotal et al., 2014; Sawyer, 1947). The weak upward motion over MIC had occurred during the early years (Fig. 9.a) and found exceeds and shifts northward during the late years as a reverse (Fig. 9.b). This reflects a strengthening in monsoon intensity, and this is consistent with the observed weakening of TEJ, which decreases upper-level divergence and leads to delayed monsoon withdrawal.

469  
470  
471  
472  
473

The strong walker circulation over the study regions in the early years (Fig. 9.c), and weakens in the late years (Fig. 9.d) are suggesting that the significant of TEJ and vertical circulation have declined, contributing to the delayed monsoon withdrawal. The reduced convective activity and moisture transport highlights how weaker jets are affecting monsoon dynamics (Roxy et al., 2015).

Formatted: Font color: Blue



474

475

476 Fig. 99 Vertical cross section of omega ( $\text{Pas}^{-1}$ ) of longitudinal averaging over ( $90^{\circ}\text{E}$ - $110^{\circ}\text{E}$ ) and latitudinal averaging ( $10^{\circ}\text{N}$ - $30^{\circ}\text{N}$ )  
 477 (a,c) for early years, (b,d) for late years. Grey dotted show the area of 95% statistically confident by t-test. This figure was created  
 478 with Python 3.10 (Matplotlib 3.5.2 [<https://matplotlib.org/>], Cartopy 0.20.0 [<https://pypi.org/project/Cartopy/>]).

479 Formatted: Caption, Don't keep with next

479

480

481

482

483

484

485

486

487

488

489

490

491

492

493

494

495

487 weakening of the 850 hPa monsoon westerlies, leading to reduced moisture convergence over the Indo-  
488 China Peninsula, as supported by the negative moisture flux convergence correlations. Furthermore,  
489 the suppressed ascending motion at mid-troposphere levels (Fig. 7,e), coupled with positive 500 hPa  
490 geopotential height anomalies (Fig. 7,f), signify the onset of mid-level atmospheric stabilization and  
491 the collapse of the monsoon thermal structure.

**Formatted:** Font color: Blue

**Formatted:** Font color: Blue

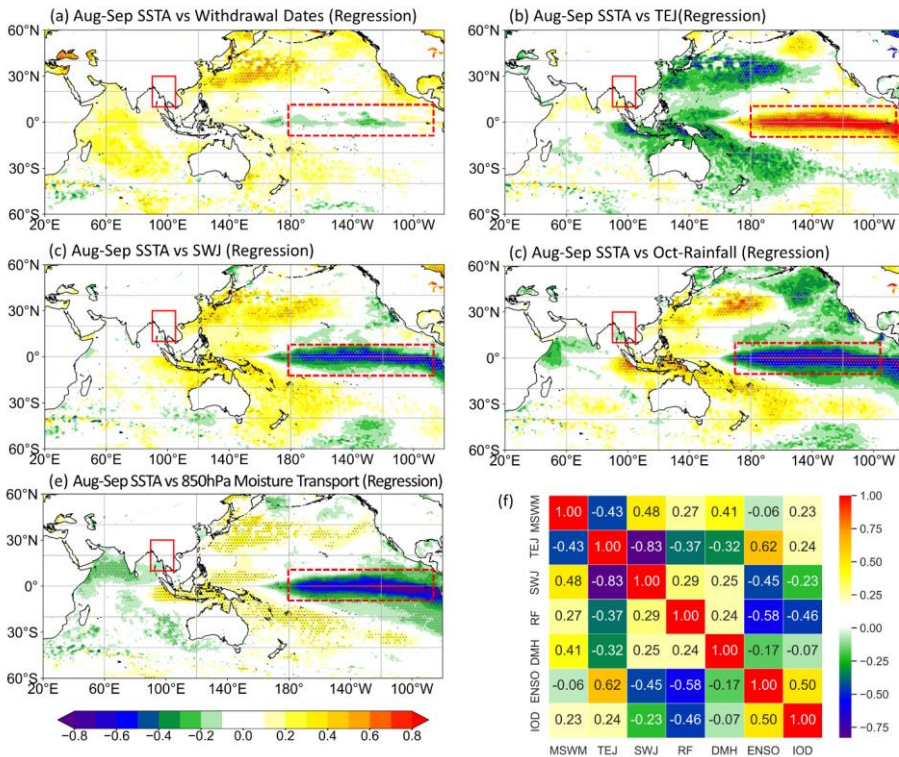
**Formatted:** Font color: Blue

**Formatted:** Font color: Blue

492 The vertical cross-sections reveal that during the late years, corresponding to delayed  
493 withdrawal events, the upper-tropospheric divergence weakens (associated with TEJ weakening),  
494 while the upper-level westerly shearing and subsidence induced by the intensified SWJ strengthen (Fig.  
495 9,c and d) This enhanced subsidence promotes tropospheric drying and suppression of convection,  
496 which together act as a dynamical brake on the monsoon system, facilitating its withdrawal.  
497 Collectively, these findings exhibited the barotropic and baroclinic adjustments in the upper-level  
498 circulation, where the interaction between the weakening TEJ and the intensifying SWJ modifies the  
499 large-scale monsoon dynamics, disrupts the monsoon Hadley circulation, and accelerates the seasonal  
500 transition toward the dry post-monsoon regime of the correlation (Fig. 7) and trend (Fig. 8) exhibited  
501 feature the critical role of atmospheric circulation patterns in influencing the delayed MSwM  
502 withdrawal. Extended moisture convergence and delayed withdrawal of monsoon systems are caused  
503 by the SWJ's strengthening and the TEJ's weakening at 200 hPa. Previous research has shown that  
504 conditions are conducive for extended monsoon motion when lower level easterlies weaken, and  
505 upper level westerlies intensify. This conclusion lends credence to those earlier findings (Krishnamurti  
506 et al., 2012; Roxy et al., 2015). In addition, prior research has demonstrated the connection between  
507 sustained moisture transport and extended convective activity with the monsoon, which is supported  
508 by the positive link between moisture flux convergence and delayed monsoon withdrawal (Goswami  
509 et al., 2006). The atmospheric dynamics anomaly, specifically the weakening of the TEJ and the  
510 intensification of the SWJ, are significant variables influencing the noted trend of delayed monsoon  
511 withdrawal.

**Formatted:** Font color: Blue

**Formatted:** Font color: Blue



512

513 Fig. 10.10 Regression between Aug-Sep Sea surface temperatures (SSTs) and (a) MSwM withdrawal dates, (b) October tropical easterly jet, (c) October sub-tropical westerly jet, (d) October rainfall over MIC and (e) October 850hPa moisture divergent. Dotted hatches mean 95% confident area by t-test statically. The red boxed show MSwM region and red dotted box show the area in the Pacific with the strongest negative positive correlation. (f) Correlation heatmap between variables used in this study. DMH refers to the MSwM withdrawal dates from National weather services recorded. This figure was created with Python 3.10 (Matplotlib 3.5.2 [https://matplotlib.org/], Cartopy 0.20.0 [https://pypi.org/project/Cartopy/]).

519 The relationship between August-September SST anomalies and the delayed withdrawal of the  
 520 MSwM showing not significant correlation over the equatorial Pacific Ocean (Fig S-9, supplementary),  
 521 indicating that negative anomaly SSTs in this region are associated with delayed monsoon withdrawal  
 522 (Fig. 10 Fig. 10.a). This is constant with the role of warm SSTs over Indochina region are maintaining  
 523 convective activity (Roxy et al., 2015; Krishnan et al., 2016) and preventing the on-time withdrawal  
 524 of the monsoon however cold SSTs over Niño3-4 region does not directly impact on withdrawal dates.  
 525 The red dotted boxed region shows the area in the Pacific with the strongest negative/positive  
 526 correlation, suggesting a link between SST anomalies in the central Pacific and the timing of monsoon  
 527 withdrawal. The relationship between SST and the tropical easterly jet (TEJ) and subtropical westerly  
 528 jet (SWJ) in October, the strong positive correlation between SST and TEJ over the Pacific Ocean (Fig  
 529 S-9.b, supplementary) suggests that warmer SSTs exceeding the strength of TEJ (Fig. 10 Fig. 10.b).

Formatted: Font color: Blue

Formatted: Font color: Blue

Formatted: Font color: Blue

530 This agreed with the previous trend and composite finding (Fig. 8Fig. 8) that the weakening of the TEJ  
531 is a critical factor in delaying the monsoon withdrawal. The weakening of the TEJ boost the lower-  
532 level monsoon circulation to endure for an extended duration over MIC (Huang et al., 2020; Sreekala  
533 et al., 2014). In contrast, Fig. 10Fig. 10.c shows a negative regression between SST and SWJ, this  
534 demonstrates that cooler SSTs over same area also strengthen the SWJ. This finding supports the idea  
535 that a positive anomalies SWJ also impact to delayed withdrawal (Dimri et al., 2015; Sreekala et al.,  
536 2014).

Formatted: Font color: Blue

537 The Aug-Sep SST of tropical Pacific and Indian ocean and rainfall within October can also  
538 predict to MIC October rainfall. The negative correlation otherwise (La Niña) in the equatorial Pacific  
539 and the negative Indian Ocean Dipole (IOD) mode are associated with exceeding rainfall over MIC  
540 (Fig. 10Fig. 10.d), which is a mark of a extended monsoon (as mentioned in Fig. 4Fig. 4). This  
541 association supports the earlier finding that increased SSTs are associated with extended rainfall during  
542 the late monsoon, especially in the central Pacific and the Indo-Pacific Warm Pool (Ghosh et al., 2009;  
543 Sabeerali et al., 2014). Furthermore, the pattern of connection associates with the impact of global  
544 climate models like the El Niño-Southern Oscillation (ENSO), which changes regional SSTs and  
545 rainfall distributions in the Indo-Pacific area.

Formatted: Font color: Blue

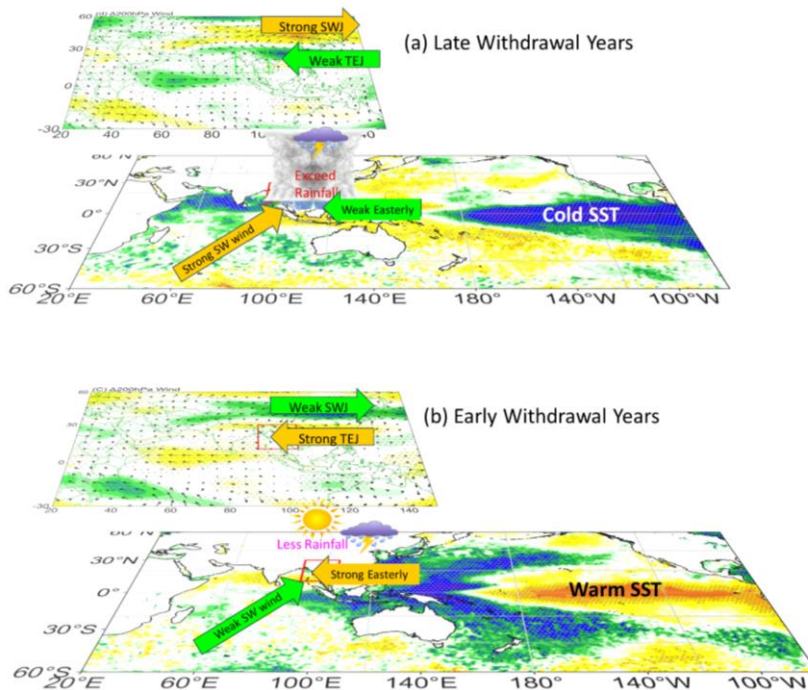
Formatted: Font color: Blue

546 To confirm this SST anomaly influence over regional rainfall or moisture flux patterns, we  
547 performed the correlation between 850-hPa moisture transport strength over MIC and Indo-Pacific  
548 SST (Fig S-9.e, supplementary). The negative regression coefficients over the central Pacific and the  
549 northern western Indian Ocean indicate that negative ENSO and IOD enhance moisture transport at  
550 lower levels (Fig. 10Fig. 10.e). However, ENSO significantly influences the monsoon onset in the  
551 Indochina region, where El Niño tends to delay onset, as seen in the central Pacific's warm SSTs  
552 positively correlated and regressed with later onset (Fig.S-10). These vice versa correlation and  
553 regression results all together point to the critical role of SSTs in driving the extended moisture  
554 convergence that maintains convective activity and delays monsoon withdrawal (Roxy et al., 2019;  
555 Sharmila et al., 2013). While this study identifies ENSO and IOD as key modulators of MSWM onset  
556 and withdrawal, emerging evidence suggests that Arctic-monsoon teleconnections may also play a role.  
557 Recent work demonstrates that MSWM intensity anomalies can drive September Arctic Sea ice  
558 variability via atmospheric bridges (Than Oo et al., 2025). Moreover, (S. Chen et al., (2024) and  
559 Cheng et al., (2025) highlight Arctic sea ice potential feedback on tropical modes (ENSO/IOD), which  
560 in turn affect monsoon dynamics. Although our analysis focuses on tropical drivers, the bidirectional  
561 nature of these interactions, particularly the Arctic's indirect influence on withdrawal via ENSO/IOD,  
562 and this should be prioritized for further investigation.

Formatted: Font color: Blue

563 In addition, the correlation matrix in [Fig. 10](#) summarizes the links among the main  
 564 variables of the research, including the MSwM withdrawal index, TEJ, SWJ, rainfall (RF), 850-hPa  
 565 moisture transport, and indices indicative of ENSO and IOD. This exhibited the anomalous SSTs,  
 566 especially in the central Pacific and northern Indian Ocean, significantly influence the intensity of the  
 567 TEJ and SWJ, as well as moisture transport and rainfall patterns. The weakened TEJ, strengthened  
 568 SWJ, and positive moisture convergence led to the well-known delay of MSwM departure ([Fig. 11](#) [Fig. 14](#)).  
 569 The results align with the current literature connecting SST anomalies, major climate models like  
 570 ENSO and IOD, and monsoon variability (Ding et al., 2011b; Jia et al., 2013; Krishnamurthy &  
 571 Kirtman, 2009). Comprehending these linkages enhances long-term predictions and prepares  
 572 agricultural systems for modifications in the southwest monsoon departure date from MIC.

**Formatted:** Font color: Blue



573  
 574 Fig. [11](#)[14](#) Air-Sea interaction Dynamical schematic of (a) late and (b) early withdrawal years. This figure was created with Python 3.10  
 575 (Matplotlib 3.5.2 [<https://matplotlib.org/>]), Cartopy 0.20.0 [<https://pypi.org/project/Cartopy/>]).

#### 576 4 Conclusion

577 Focusing on the timing of the monsoon onset and withdrawal, the study offers vital insights into  
 578 the changing dynamics and interannual variability of the Mainland Indochina Southwest Monsoon

579 (MSwM). With the development of the Cumulative Change of the MSwM (CPM) index, a more  
580 thorough knowledge of monsoon transitions may be achieved than with typical daily measurements.  
581 This index effectively captures the continuous build-up of crucial atmospheric components.

582 Withdrawal timing has been noticeably delayed over the past few decades, according to the  
583 findings, which also show clear patterns in the start and withdrawal phases. SWJ and the TEJ, which  
584 control the monsoon withdrawal processes, have had a significant impact on this delay. Additionally,  
585 the MSwM atmospheric circulation and moisture transport are significantly influenced by SST  
586 anomalies, especially in the western Pacific and Indian Oceans. In mainland Indochina, extended  
587 monsoon seasons increase the risk of flooding and interfere with agricultural cycles, underscoring the  
588 urgent need for efficient water management and flexible farming techniques.

589 As conclusion, the MSwM CPM index is a great tool for tracking monsoon variability, and the  
590 framework it gives for studying how climate change is affecting the regional monsoon system through  
591 composite correlation and trend analysis is invaluable. Improving our understanding of monsoon  
592 behavior and constructing more accurate prediction models will require further studies, specifically on  
593 the teleconnection mechanisms between large-scale climatic drivers (such ENSO and IOD) and  
594 MSwM.

595 **Data Availability**

596 **Source Data**

597 All Reanalysis rainfall, wind components, OLR, and Mean Seal Level Pressure netcdf4 data for this  
598 study were downloaded from the NCEP and ECMWF data portal.

599 The historical record of onset and withdrawal dates by DMH of Myanmar the actual monthly rainfall  
600 observation data and mean sea level pressure data from 79 observation stations used to support the  
601 findings of this study was provided under permission by Myanmar's Department of Meteorology and  
602 Hydrology (DMH) and hence cannot be freely distributed. Requests for access to these data should be  
603 made to the Director-General of DMH, Myanmar. <https://www.moezala.gov.mm/>

604 **Software availability**

605 Open Grads (<http://opengrads.org/>), Climate data operator (<https://code.mpimet.mpg.de/>), Python and  
606 IBM SPSS are mainly used for this study. Among these first two are open-source applications for  
607 everyone. Codes are also available upon request.

608 **Conflicts of Interest**

609 I declared that there is no potential conflict of interest with any of the following statements.

- 610 1. For any component of the submitted work, the author received no cash or services from a third  
611 party (government, commercial, private foundation, etc). (including but not limited to grants,  
612 data monitoring board, study design, manuscript preparation, statistical analysis, etc.).
- 613 2. The author is not affiliated with any entity that has a direct or indirect financial interest in the  
614 manuscript's subject matter.
- 615 3. The author was involved in the following aspects of the project: (a) idea and design, or data  
616 analysis and interpretation; (b) authoring the article or critically reviewing it for essential  
617 intellectual content; and (c) approval of the final version.
- 618 4. This work has not been submitted to, and is not currently being reviewed by, any other journal  
619 or publishing venue.
- 620 5. The author has no patents that are broadly relevant to the work, whether proposed, pending, or  
621 issued.
- 622 6. The author received no payment or services from a third party for any aspect of the submitted  
623 work (government, commercial, private foundation, etc). (including but not limited to grants,  
624 data monitoring board, study design, manuscript preparation, statistical analysis, etc.).

625 **Funding Statement**

626 This study is supported by the National Natural Science Foundation of China (Grant 42088101).

627 **Acknowledgment**

628 The researcher expresses special thanks to all Professors who approve and support this research  
629 and Nanjing University of Information Science for support to come out of this research. I would also  
630 like to extend my gratitude to Professor Haishan Chen from Nanjing University of Information Science  
631 and Technology, for supervisor this paper and his others, support during this research. The author  
632 acknowledges heartfelt thanks to the scientists of the ECMFW for supporting ERA5 datasets and the  
633 Department of Meteorology and Hydrology for support the data of Myanmar. Additionally, the author  
634 would like to thank three reviewers for their constructive and insightful reviews and comments which  
635 have significantly helped to improve the manuscript. First author Kyaw Than Oo would like to show  
636 his gratitude to Mrs Moh Moh Zaw Thin from UIBE, China and Mr. Phyto Sitt Thyn Kyaw for her  
637 physical and mental support for this work.

638 **Author Contribution**

639 **Kyaw Than Oo:** Conceptualization, methodology, data curation, writing- original draft preparation.,  
640 visualization and investigation.

641 **Haishan Chen:** Supervision.

642 **Kazora Jonah:** Writing – review & editing.

643 **Xinguan Du:** Writing – review & editing.

644

645

646 **References**

647 Ajayamohan, R. S., Rao, S. A., Luo, J. J., & Yamagata, T. (2009). Influence of Indian Ocean Dipole  
648 on boreal summer intraseasonal oscillations in a coupled general circulation model. *Journal of*  
649 *Geophysical Research Atmospheres*, 114(6). <https://doi.org/10.1029/2008JD011096>

650 Akter, N., & Tsuboki, K. (2014). Role of synoptic scale forcing in cyclogenesis over the Bay of Bengal.  
651 *Climate Dynamics*, 43(9–10), 2651–2662. <https://doi.org/10.1007/S00382-014-2077-9>  
652 METRICS

653 Aung, L. L., Zin, E. E., Theingi, P., Elvera, N., Aung, P. P., Han, T. T., Oe, Y., & Skaland, R. G.  
654 (2017). Myanmar Climate Report. Norwegian Meteorological Institute, 9, 105.

655 Bombardi, R. J., Kinter, J. L., & Frauenfeld, O. W. (2019). A global gridded dataset of the  
656 characteristics of the rainy and dry seasons. *Bulletin of the American Meteorological Society*,  
657 100(7), 1315–1328. <https://doi.org/10.1175/BAMS-D-18-0177.1>

658 Bordoni, S., & Schneider, T. (2008). Monsoons as eddy mediated regime transitions of the tropical  
659 overturning circulation. *Nature Geoscience*, 1(8), 515–519. <https://doi.org/10.1038/NGEO248>

660 Breiman, L. (2001). Random forests. *Machine Learning*, 45(1), 5–32.  
661 <https://doi.org/10.1023/A:1010933404324>

662 Cao, J., Hu, J., & Tao, Y. (2012). An index for the interface between the Indian summer monsoon and

663 the East Asian summer monsoon. *Journal of Geophysical Research Atmospheres*, 117(17), 1–9.  
664 <https://doi.org/10.1029/2012JD017841>

665 Chen, L., Chen, W., Hu, P., Chen, S., & An, X. (2023). Climatological characteristics of the East Asian  
666 summer monsoon retreat based on observational analysis. *Climate Dynamics*, 60(9–10), 3023–  
667 3037. <https://doi.org/10.1007/s00382-022-06489-6>

668 Chen, M., Shi, W., Xie, P., Silva, V. B. S., Kousky, V. E., Higgins, R. W., & Janowiak, J. E. (2008).  
669 Assessing objective techniques for gauge-based analyses of global daily precipitation. *Journal of  
670 Geophysical Research Atmospheres*, 113(4). <https://doi.org/10.1029/2007JD009132>

671 Chen, S., Chen, W., Zhou, W., Wu, R., Ding, S., Chen, L., He, Z., & Yang, R. (2024). Interdecadal  
672 Variation in the Impact of Arctic Sea Ice on El Niño–Southern Oscillation: The Role of  
673 Atmospheric Mean Flow. *Journal of Climate*, 37(21), 5483–5506. <https://doi.org/10.1175/JCLI-D-23-0733.1>

675 Cheng, X., Chen, S., Chen, W., Wu, R., Ding, S., Zhou, W., Wang, L., Yang, Y., Piao, J., & Hu, P.  
676 (2025). Interdecadal Variation in the Impact of Arctic Sea Ice on El Niño–Southern Oscillation:  
677 The Role of Atmospheric Mean Flow. *Journal of Climate*, 38(13), 3109–3129.  
678 <https://doi.org/10.1175/JCLI-D-24-0419.1>

679 Chou, C., Neelin, J. D., Chen, C. A., & Tu, J. Y. (2009). Evaluating the “rich get richer” mechanism  
680 in tropical precipitation change under global warming. *Journal of Climate*, 22(8), 1982–2005.  
681 <https://doi.org/10.1175/2008JCLI2471.1>

682 Colbert, A. J., Soden, B. J., & Kirtman, B. P. (2015). The impact of natural and anthropogenic climate  
683 change on western North Pacific tropical cyclone tracks. *Journal of Climate*, 28(5), 1806–1823.  
684 <https://doi.org/10.1175/JCLI-D-14-00100.1>

685 CY Li, L. Z. (1999). Activity of the South China Sea summer monsoon and its effect. *Acta Atmos Sinica*,  
686 23, 257–266.

687 Dimri, A. P., Niyogi, D., Barros, A. P., Ridley, J., Mohanty, U. C., Yasunari, T., & Sikka, D. R. (2015).  
688 Reviews of Geophysics: Western Disturbances: A review. *Reviews of Geophysics*, 53, 225–246.  
689 <https://doi.org/10.1002/2014RG000460>. Received

690 Ding, Q., Wang, B., Wallace, J. M., & Branstator, G. (2011a). Tropical extratropical teleconnections  
691 in boreal summer: Observed interannual variability. *Journal of Climate*, 24(7), 1878–1896.  
692 <https://doi.org/10.1175/2011JCLI3621.1>

693 Ding, Q., Wang, B., Wallace, J. M., & Branstator, G. (2011b). Tropical extratropical teleconnections  
694 in boreal summer: Observed interannual variability. *Journal of Climate*, 24(7), 1878–1896.  
695 <https://doi.org/10.1175/2011JCLI3621.1>

696 Evan, A. T., & Camargo, S. J. (2011). A climatology of Arabian Sea cyclonic storms. *J Clim*, 24(1),  
697 140–158. <https://doi.org/10.1175/2010JCLI3611.1>

698 Fasullo, J., & Webster, P. J. (2003). A hydrological definition of Indian Monsoon onset and withdrawal.  
699 *Journal of Climate*, 16(19), 3200–3211. [https://doi.org/10.1175/1520-0442\(2003\)016<3200:AHDOI>2.0.CO;2](https://doi.org/10.1175/1520-0442(2003)016<3200:AHDOI>2.0.CO;2)

700 Fesu, B. O., & Wang, S. Y. S. (2015). Bay of Bengal: coupling of pre-monsoon tropical cyclones with  
701 the monsoon onset in Myanmar. *Climate Dynamics*, 45(3–4), 697–709.  
702 <https://doi.org/10.1007/s00382-014-2289-z>

703 Ghosh, S., Luniya, V., & Gupta, A. (2009). Trend analysis of Indian summer monsoon rainfall at  
704 different spatial scales. *Atmospheric Science Letters*, 10(4), 285–290.  
705 <https://doi.org/10.1002/ASL.235>

706

707 Gill, A. E. (1980). Some simple solutions for heat induced tropical circulation. *Quarterly Journal of*  
708 *the Royal Meteorological Society*, 106(449), 447–462. <https://doi.org/10.1002/qj.49710644905>

709 Goswami, B. N., Krishnamurthy, V., & Annamalai, H. (1999). A broad scale circulation index for the  
710 interannual variability of the Indian summer monsoon. *Quarterly Journal of the Royal*  
711 *Meteorological Society*, 125(554), 611–633. <https://doi.org/10.1002/qj.49712555412>

712 Goswami, B. N., & Xavier, P. K. (2005). ENSO control on the south Asian monsoon through the  
713 length of the rainy season. *Geophys Res Lett*, 32(18), L18717.  
714 <https://doi.org/10.1029/2005gl023216>

715 Hannachi, A. (2004). A primer for EOF analysis of climate data. *Reading: University of Reading*, 1–  
716 33. [http://www.o3d.org/eas\\_6490/lectures/EOFs/eofprimer.pdf](http://www.o3d.org/eas_6490/lectures/EOFs/eofprimer.pdf)

717 Hersbach, H., Bell, B., Berrisford, P., Hirahara, S., Horányi, A., Muñoz-Sabater, J., Nicolas, J., Peubey,  
718 C., Radu, R., Schepers, D., Simmons, A., Soci, C., Abdalla, S., Abellan, X., Balsamo, G.,  
719 Bechtold, P., Biavati, G., Bidlot, J., Bonavita, M., ... Thépaut, J. N. (2020). The ERA5 global  
720 reanalysis. *Quarterly Journal of the Royal Meteorological Society*, 146(730), 1999–2049.  
721 <https://doi.org/10.1002/qj.3803>

722 Htway, O., & Matsumoto, J. (2011). Climatological onset dates of summer monsoon over Myanmar.  
723 *International Journal of Climatology*, 31(3), 382–393. <https://doi.org/10.1002/ijoc.2076>

724 Hu, P., Chen, S., Chen, W., & Tan, B. (2025). Asian Pacific Summer Monsoon Variability and  
725 Atmospheric Teleconnection Patterns: Review and Outlook. *Journal of Meteorological Research*,  
726 39(3), 651–672. <https://doi.org/10.1007/s13351-025-4222-2>

727 Hu, P., Chen, W., Chen, S., & Huang, R. (2019). Interannual variability and triggers of the South China  
728 Sea summer monsoon withdrawal. *Climate Dynamics*, 53(7–8), 4355–4372.  
729 <https://doi.org/10.1007/s00382-019-04790-5>

730 Hu, P., Chen, W., Chen, S., Liu, Y., & Huang, R. (2020). Extremely Early Summer Monsoon Onset  
731 in the South China Sea in 2019 Following an El Niño Event. *Monthly Weather Review*, 148(5),  
732 1877–1890. <https://doi.org/10.1175/MWR-D-19-0317.1>

733 Hu, P., Chen, W., Wang, L., Chen, S., Liu, Y., & Chen, L. (2022). Revisiting the ENSO monsoonal  
734 rainfall relationship: new insights based on an objective determination of the Asian summer  
735 monsoon duration. *Environmental Research Letters*, 17(10). <https://doi.org/10.1088/1748-9326/ae97ad>

737 Huang, S., Wang, B., & Wen, Z. (2020). Dramatic weakening of the tropical easterly jet projected by  
738 CMIP6 models. *Journal of Climate*, 33(19), 8439–8455. <https://doi.org/10.1175/JCLI-D-19-1002.1>

740 Jia, X., Yang, S., Li, X., Liu, Y., Wang, H., Liu, X., & Weaver, S. (2013). Prediction of global patterns  
741 of dominant quasi biweekly oscillation by the NCEP Climate Forecast System version 2. *Climate*  
742 *Dynamics*, 11(5–6), 1635–1650. <https://doi.org/10.1007/S00382-013-1877-7>

743 Jiao, D., Xu, N., Yang, F., & Xu, K. (2021). Evaluation of spatial temporal variation performance of  
744 ERA5 precipitation data in China. *Scientific Reports*, 11(1), 1–13.  
745 <https://doi.org/10.1038/s41598-021-97432-y>

746 K Lau, K. K. S. Y. (2000). Dynamical and boundary forcing characteristics of regional components of  
747 the Asian summer monsoon. *J. Clim.*, 13, 2461–2482. [https://doi.org/10.1175/1520-0442\(2000\)013<2461:dabfco>2.0.co](https://doi.org/10.1175/1520-0442(2000)013<2461:dabfco>2.0.co)

749 Kanamitsu, M., Ebisuzaki, W., Woollen, J., Yang, S. K., Hnilo, J. J., Fiorino, M., & Potter, G. L.  
750 (2002). NCEP–DOE AMIP II reanalysis (R–2). *Bulletin of the American Meteorological Society*,

751 83(11). <https://doi.org/10.1175/BAMS-83-11-1631>

752 Kotal, S. D., Bhattacharya, S. K., Roy Bhownik, S. K., & Kundu, P. K. (2014). Growth of cyclone  
753 Viyaru and Phailin - A comparative study. *J. Earth Syst. Sci.*, 123(7), 1619–1635.  
754 <https://doi.org/10.1007/s12040-014-0493-1>

755 Krishnamurthy, V., & Kirtman, B. P. (2009). Relation between Indian monsoon variability and SST.  
756 *Journal of Climate*, 22(17), 4437–4458. <https://doi.org/10.1175/2009JCLI2520.1>

757 Krugman, P. R., Obstfeld, M., & Melitz, M. J. T. A. T. T. (2018). *International economics : theory  
& policy* (Eleventh ed.). Pearson New York. <https://doi.org/LK>  
758 <https://worldcat.org/title/1014329502>

760 Li, H., Dai, A., Zhou, T., & Lu, J. (2010). Responses of East Asian summer monsoon to historical SST  
761 and atmospheric forcing during 1950–2000. *Climate Dynamics*, 34(4), 501–514.  
762 <https://doi.org/10.1007/S00382-008-0482-7>

763 Liu, Y., Cook, K. H., & Vizy, E. K. (2021). Delayed retreat of the summer monsoon over the Indochina  
764 Peninsula linked to surface warming trends. *International Journal of Climatology*, 41(3), 1927–  
765 1938. <https://doi.org/10.1002/IJC.6938>

766 Loikith, P. C., Pampush, L. A., Slinskey, E., Detzer, J., Meehoso, C. R., & Barkhordarian, A. (2019).  
767 A climatology of daily synoptic circulation patterns and associated surface meteorology over  
768 southern South America. *Climate Dynamics*, 53(7–8), 4019–4035.  
769 <https://doi.org/10.1007/S00382-019-04768-3/FIGURES/12>

770 Ma, Y. Z. (2019). Quantitative Geosciences: Data Analytics, Geostatistics, Reservoir Characterization  
771 and Modeling. In *Quantitative Geosciences: Data Analytics, Geostatistics, Reservoir  
772 Characterization and Modeling*. <https://doi.org/10.1007/978-3-030-17860-4>

773 Mao, J., & Wu, G. (2007). Interannual variability in the onset of the summer monsoon over the Eastern  
774 Bay of Bengal. *Theoretical and Applied Climatology*, 89(3–4), 155–170.  
775 <https://doi.org/10.1007/S00704-006-0265-1>

776 Oo, K. T. (2021). How El Nino / La Nina & India Ocean Dipole ( IDO ) Influence on Myanmar  
777 Rainfall Distribution ( Statistical Analysis Report ) ( 1990–2019 ). *J Environ Sci.* 2021, 17(1),  
778 178. <https://doi.org/10.37532/environmental.science.2021.17.178>

779 Oo, K. T. (2022a). Interannual Variability of Winter Rainfall in Upper Myanmar. *Journal of  
780 Sustainability and Environmental Management*, 1(3), 344–358.  
781 <https://doi.org/10.3126/josem.v1i3.48001>

782 Oo, K. T. (2022b). Interannual Variability of Winter Rainfall in Upper Myanmar. *Journal of  
783 Sustainability and Environmental Management*, 1(3), 344–358.  
784 <https://doi.org/10.3126/JOSEM.V1I3.48001>

785 Oo, K. T. (2022c). Interannual Variability of Winter Rainfall in Upper Myanmar. *Journal of  
786 Sustainability and Environmental Management*, 1(3), 344–358.  
787 <https://doi.org/https://doi.org/10.3126/josem.v1i3.48001>

788 Oo, K. T. (2023a). Climatology Definition of the Myanmar Southwest Monsoon (MSwM): Change  
789 Point Index (CPI). *Advances in Meteorology*, 2023, 2346975.  
790 <https://doi.org/10.1155/2023/2346975>

791 Oo, K. T. (2023b). Climatology Definition of the Myanmar Southwest Monsoon (MSwM): Change  
792 Point Index (CPI). *Advances in Meteorology*, 2023, 2346975.  
793 <https://doi.org/10.1155/2023/2346975>

794 Oo, K. T., Chen, H., Dong, Y., & Jonah, K. (2024). Investigating the link between Mainland Indochina  
795 monsoon onset dates and cyclones over the Bay of Bengal basin. *Climate Dynamics*.  
796 <https://doi.org/10.1007/S00382-024-07342-8>

797 Oo, K. T., Dalhatu, A., Jonah, K., Dong, Y., & Madhushanka, D. (2025). Examining of interannual  
798 variability in the Mainland Indochina Southwest Monsoon onset applying new monsoon index.  
799 *Theoretical and Applied Climatology*. <https://doi.org/10.1007/s00704-025-05543-7>

800 Oo, K. T., & Jonah, K. (2024). Interannual variation of summer southwest monsoon rainfall over the  
801 monsoon core regions of the eastern Bay of Bengal and its relationship with oceans. *Journal of*  
802 *Atmospheric and Solar-Terrestrial Physics*, 265, 106341.  
803 <https://doi.org/10.1016/J.JASTP.2024.106341>

804 Q-Guo, J. W. (1988). A comparison of the summer precipitation in India with that in China. *J. Trop.*  
805 *Meteorol.*, 1, 53–60.

806 Ramage, C. S. (1971). *Monsoon meteorology*. Academic Press.

807 Ren, Q., Liu, F., Wang, B., Yang, S., Wang, H., & Dong, W. (2022). Origins of the Intraseasonal  
808 Variability of East Asian Summer Precipitation. *Geophysical Research Letters*, 49(4).  
809 <https://doi.org/10.1029/2021GL096574>

810 Roxy, M. K., Dasgupta, P., McPhaden, M. J., Suematsu, T., Zhang, C., & Kim, D. (2019). Twofold  
811 expansion of the Indo-Pacific warm pool warps the MJO life cycle. *Nature*, 575(7784), 647–651.  
812 <https://doi.org/10.1038/s41586-019-1764-4>

813 Roxy, M. K., Ritika, K., Terray, P., & Masson, S. (2014). The curious case of Indian Ocean warming.  
814 *Journal of Climate*, 27(22), 8501–8509. <https://doi.org/10.1175/JCLI-D-14-00471.1>

815 Sabeerali, C. T., Rao, S. A., George, G., Nagarjuna Rao, D., Mahapatra, S., Kulkarni, A., &  
816 Murtugudde, R. (2014). Modulation of monsoon intraseasonal oscillations in the recent warming  
817 period. *Journal of Geophysical Research*, 119(9), 5185–5203.  
818 <https://doi.org/10.1002/2013JD021261>

819 Salinger, M. J., Shrestha, M. L., Ailikun, Dong, W., McGregor, J. L., & Wang, S. (2014). Climate in  
820 Asia and the Pacific: Climate Variability and Change. *Advances in Global Change Research*, 56,  
821 17–57. [https://doi.org/10.1007/978-94-007-7338-7\\_2](https://doi.org/10.1007/978-94-007-7338-7_2)

822 Sawyer, J. S. (1947). The structure of the intertropical front over N.W. India during the S.W. Monsoon.  
823 *Quarterly Journal of the Royal Meteorological Society*, 73(317–318), 346–369.  
824 <https://doi.org/10.1002/QJ.49707331709>

825 Schmidhammer. (2000). Box Plot and Robust Statistics. *Matrix*, 5, 109–122.

826 Seager, R., Naik, N., & Veechi, G. A. (2010). Thermodynamic and dynamic mechanisms for large-  
827 scale changes in the hydrological cycle in response to global warming. *Journal of Climate*, 23(17),  
828 4651–4668. <https://doi.org/10.1175/2010JCLI3655.1>

829 Selman, C., & Misra, V. (2014). The Met Office Hadley Centre sea ice and sea surface temperature  
830 data set, version 2: 1. Sea ice concentrations. *Journal of Geophysical Research*, 3, 180–198.  
831 <https://doi.org/10.1002/2013JD021040>. Received

832 Sharmila, S., Pillai, P. A., Joseph, S., Roxy, M., Krishna, R. P. M., Chattopadhyay, R., Abhilash, S.,  
833 Sahai, A. K., & Goswami, B. N. (2013). Role of ocean atmosphere interaction on northward  
834 propagation of Indian summer monsoon intra seasonal oscillations (MISO). *Climate Dynamics*,  
835 41(5–6), 1651–1669. <https://doi.org/10.1007/S00382-013-1854-4>

836 Song, L., Hu, P., Chen, W., Yang, R., Ma, T., & Zheng, Y. (2025). Increasing Trend of Summer

837 Monsoonal Rainfall Tied to the Extension of the South China Sea Summer Monsoon Duration.  
838 *Atmospheric Science Letters*, 26(7), 1–9. <https://doi.org/10.1002/asl.1308>

839 Sreekala, P. P., Bhaskara Rao, S. V., Arunachalam, M. S., & Harikiran, C. (2014). A study on the  
840 decreasing trend in tropical easterly jet stream (TEJ) and its impact on Indian summer monsoon  
841 rainfall. *Theoretical and Applied Climatology*, 118(1–2), 107–114.  
842 <https://doi.org/10.1007/s00704-013-1049-z>

843 Than Oo, K., Datti, A. D., Jonah, K., & Ayugi, B. O. (2025). The Complex Teleconnections and  
844 Feedback Mechanisms between Mainland Indochina's Southwest Monsoon and Arctic Ocean  
845 Climate Variability. *EGUphere*, 2025, 1–32. <https://doi.org/10.5194/eguphphere-2025-521>

846 Vijaya Kumari, K., Karuna Sagar, S., Viswanadhapalli, V., Dasari, H. P., & Bhaskara Rao, S. V. (2018).  
847 Role of planetary boundary layer processes on the simulation of tropical cyclones over Bay of  
848 Bengal. *Pure and Applied Geophysics*, 176(2), 951–977. <https://doi.org/10.1007/s00021-018-2017-4>

849 Walker, J. M., Bordoni, S., & Schneider, T. (2015). Interannual variability in the large scale dynamics  
850 of the South Asian summer monsoon. *Journal of Climate*, 28(9), 3731–3750.  
851 <https://doi.org/10.1175/JCLI-D-14-00612.1>

852 Wang, B., & Ho, L. (2002). Rainy season of the Asian Pacific summer monsoon. *Journal of Climate*,  
853 15(4), 386–398. [https://doi.org/10.1175/1520-0442\(2002\)015<0386:RSOTAP>2.0.CO;2](https://doi.org/10.1175/1520-0442(2002)015<0386:RSOTAP>2.0.CO;2)

854 Wang, B., Huang, F., Wu, Z., Yang, J., Fu, X., & Kikuchi, K. (2009). Multi-scale climate variability  
855 of the South China Sea monsoon: A review. *Dynamics of Atmospheres and Oceans*, 47(1), 15–  
856 37. <https://doi.org/https://doi.org/10.1016/j.dynatmocce.2008.09.004>

857 Wang, B., LinHo, Zhang, Y., & Lu, M. M. (2004). Definition of South China Sea monsoon onset and  
858 commencement of the East Asian summer monsoon. *Journal of Climate*, 17(4), 699–710.  
859 <https://doi.org/10.1175/2932.1>

860 Wang, B., Wu, R., & Lau, K. M. (2001). Interannual variability of the Asian summer monsoon:  
861 Contrasts between the Indian and the Western North Pacific East Asian monsoons. *Journal of Climate*,  
862 14(20), 4073–4090. [https://doi.org/10.1175/1520-0442\(2001\)014<4073:IVOTAS>2.0.CO;2](https://doi.org/10.1175/1520-0442(2001)014<4073:IVOTAS>2.0.CO;2)

863 Wang, B., Wu, Z., Li, J., Liu, J., Chang, C. P., Ding, Y., & Wu, G. (2008). How to measure the strength  
864 of the East Asian summer monsoon. *Journal of Climate*, 21(17), 4449–4463.  
865 <https://doi.org/10.1175/2008JCLI2183.1>

866 Wang, X., & Zhou, W. (2024). Interdecadal variation of the monsoon trough and its relationship with  
867 tropical cyclone genesis over the South China Sea and Philippine Sea around the mid-2000s.  
868 *Climate Dynamics*, 62(5), 3743–3762. <https://doi.org/10.1007/s00382-023-07096-9>

869 Webster, P. J., & Yang, S. (1992). Monsoon and El Niño: Selectively Interactive Systems. *Quarterly  
870 Journal of the Royal Meteorological Society*, 118(507), 877–926.  
871 <https://doi.org/10.1002/qj.49711850705>

872 Win Zin, W., & Rutten, M. (2017). Long term Changes in Annual Precipitation and Monsoon Seasonal  
873 Characteristics in Myanmar. *Hydrology: Current Research*, 08(02). <https://doi.org/10.4172/2157-7587.1000271>

874 Wu, R. (2017). Relationship between Indian and East Asian summer rainfall variations. *Advances in  
875 Atmospheric Sciences*, 34(1), 4–15. <https://doi.org/10.1007/S00376-016-6216-6>

876 Wu, X., & Mao, J. (2018). Spatial and interannual variations of spring rainfall over eastern China in  
877 association with PDO–ENSO events. *Theoretical and Applied Climatology*, 134(3–4), 935–953.  
878 <https://doi.org/10.1007/s00704-017-1880-0>

879

880

881 <https://doi.org/10.1007/s00704-017-2323-2>

882 Xing, N., Li, J., & Wang, L. (2016). Effect of the early and late onset of summer monsoon over the  
883 Bay of Bengal on Asian precipitation in May. *Climate Dynamics*, 47(5–6), 1961–1970.  
884 <https://doi.org/10.1007/s00382-015-2944-z>

885 Xu, C., Wang, S., Borhara, K., Buckley, B., Tan, N., Zhao, Y., An, W., Sano, M., Nakatsuka, T.,  
886 & Guo, Z. (2023). Asian Australian summer monsoons linkage to ENSO strengthened by global  
887 warming. *Npj Climate and Atmospheric Science*, 6(1). <https://doi.org/10.1038/S41612-023-00341-2>

888 Zhang, H., Liang, P., Moise, A., & Hanson, L. (2012). Diagnosing potential changes in Asian summer  
889 monsoon onset and duration in IPCC AR4 model simulations using moisture and wind indices.  
890 *Climate Dynamics*, 39(9–10), 2465–2486. <https://doi.org/10.1007/s00382-012-1289-0>

891 Zhang, S., Qu, X., Huang, G., Hu, P., Zhou, S., & Wu, L. (2024). Delayed Onset of Indian Summer  
892 Monsoon in Response to CO<sub>2</sub> Removal. *Earth's Future*, 12(2), 1–17.  
893 <https://doi.org/10.1029/2023EF004039>

894 Zhang, Y., Li, T., Wang, B., & Wu, G. (2002a). Onset of the summer monsoon over the Indochina  
895 Peninsula: Climatology and interannual variations. *Journal of Climate*, 15(22), 3206–3221.  
896 [https://doi.org/10.1175/1520-0442\(2002\)015<3206:OOTSMO>2.0.CO;2](https://doi.org/10.1175/1520-0442(2002)015<3206:OOTSMO>2.0.CO;2)

897 Zhang, Y., Li, T., Wang, B., & Wu, G. (2002b). Onset of the Summer Monsoon over the Indochina  
898 Peninsula: Climatology and Interannual Variations. *Journal of Climate*, 15(22), 3206–3221.  
899 [https://doi.org/https://doi.org/10.1175/1520-0442\(2002\)015<3206:OOTSMO>2.0.CO;2](https://doi.org/https://doi.org/10.1175/1520-0442(2002)015<3206:OOTSMO>2.0.CO;2)

900 Zin Mie Mie Sein, B., Ogwang, V., Ongoma, Faustin Katehele Ogov, & Kpaikpai Batebana. (2015).  
901 *Inter annual variability of Summer Monsoon Rainfall over Myanmar in relation to IOD and  
902 ENSO* (pp. 4:28–36). *Journal of Environmental and Agricultural Sciences*.

903 Ajayamohan, R. S., Rao, S. A., Luo, J. J., & Yamagata, T. (2009). Influence of Indian Ocean Dipole  
904 on boreal summer intraseasonal oscillations in a coupled general circulation model. *Journal of  
905 Geophysical Research Atmospheres*, 114(6). <https://doi.org/10.1029/2008JD011096>

906 Akter, N., & Tsuboki, K. (2014). Role of synoptic-scale forcing in cyclogenesis over the Bay of Bengal.  
907 *Climate Dynamics*, 43(9–10), 2651–2662. [https://doi.org/10.1007/S00382-014-2077-9/METRICS](https://doi.org/10.1007/S00382-014-2077-9)

908 Aung, L. L., Zin, E. E., Theingi, P., Elvera, N., Aung, P. P., Han, T. T., Oo, Y., & Skaland, R. G.  
909 (2017). Myanmar Climate Report. *Norwegian Meteorological Institute*, 9, 105.

910 Bombardi, R. J., Kinter, J. L., & Frauenfeld, O. W. (2019). A global gridded dataset of the  
911 characteristics of the rainy and dry seasons. *Bulletin of the American Meteorological Society*,  
912 100(7), 1315–1328. <https://doi.org/10.1175/BAMS-D-18-0177.1>

913 Bordoni, S., & Schneider, T. (2008). Monsoons as eddy-mediated regime transitions of the tropical  
914 overturning circulation. *Nature Geoscience*, 1(8), 515–519. <https://doi.org/10.1038/NGEO248>

915 Breiman, L. (2001). Random forests. *Machine Learning*, 45(1), 5–32.  
916 <https://doi.org/10.1023/A:1010933404324>

917 Cao, J., Hu, J., & Tao, Y. (2012). An index for the interface between the Indian summer monsoon and  
918 the East Asian summer monsoon. *Journal of Geophysical Research Atmospheres*, 117(17), 1–9.  
919 <https://doi.org/10.1029/2012JD017841>

920 Chen, L., Chen, W., Hu, P., Chen, S., & An, X. (2023). Climatological characteristics of the East Asian  
921 summer monsoon retreat based on observational analysis. *Climate Dynamics*, 60(9–10), 3023–  
922

924 3037. <https://doi.org/10.1007/s00382-022-06489-6>

925 Chen, M., Shi, W., Xie, P., Silva, V. B. S., Kousky, V. E., Higgins, R. W., & Janowiak, J. E. (2008).  
926 Assessing objective techniques for gauge-based analyses of global daily precipitation. *Journal of*  
927 *Geophysical Research Atmospheres*, 113(4). <https://doi.org/10.1029/2007JD009132>

928 Chen, S., Chen, W., Zhou, W., Wu, R., Ding, S., Chen, L., He, Z., & Yang, R. (2024). Interdecadal  
929 Variation in the Impact of Arctic Sea Ice on El Niño–Southern Oscillation: The Role of  
930 Atmospheric Mean Flow. *Journal of Climate*, 37(21), 5483–5506. <https://doi.org/10.1175/JCLI-D-23-0733.1>

931 Cheng, X., Chen, S., Chen, W., Wu, R., Ding, S., Zhou, W., Wang, L., Yang, Y., Piao, J., & Hu, P.  
932 (2025). Interdecadal Variation in the Impact of Arctic Sea Ice on El Niño–Southern Oscillation:  
933 The Role of Atmospheric Mean Flow. *Journal of Climate*, 38(13), 3109–3129.  
934 <https://doi.org/10.1175/JCLI-D-24-0419.1>

935 Chou, C., Neelin, J. D., Chen, C. A., & Tu, J. Y. (2009). Evaluating the “rich-get-richer” mechanism  
936 in tropical precipitation change under global warming. *Journal of Climate*, 22(8), 1982–2005.  
937 <https://doi.org/10.1175/2008JCLI2471.1>

938 Colbert, A. J., Soden, B. J., & Kirtman, B. P. (2015). The impact of natural and anthropogenic climate  
939 change on western North Pacific tropical cyclone tracks. *Journal of Climate*, 28(5), 1806–1823.  
940 <https://doi.org/10.1175/JCLI-D-14-00100.1>

941 CY Li, L. Z. (1999). Activity of the South China Sea summer monsoon and its effect. *Acta Atmos Sinica*,  
942 23, 257–266.

943 Dimri, A. P., Niyogi, D., Barros, A. P., Ridley, J., Mohanty, U. C., Yasunari, T., & Sikka, D. R. (2015).  
944 Reviews of Geophysics Western Disturbances: A review. *Reviews of Geophysics*, 53, 225–246.  
945 <https://doi.org/10.1002/2014RG000460>. Received

946 Ding, Q., Wang, B., Wallace, J. M., & Branstator, G. (2011a). Tropical-extratropical teleconnections  
947 in boreal summer: Observed interannual variability. *Journal of Climate*, 24(7), 1878–1896.  
948 <https://doi.org/10.1175/2011JCLI3621.1>

949 Ding, Q., Wang, B., Wallace, J. M., & Branstator, G. (2011b). Tropical-extratropical teleconnections  
950 in boreal summer: Observed interannual variability. *Journal of Climate*, 24(7), 1878–1896.  
951 <https://doi.org/10.1175/2011JCLI3621.1>

952 Evan, A. T., & Camargo, S. J. (2011). A climatology of Arabian Sea cyclonic storms. *J Clim*, 24(1),  
953 140–158. <https://doi.org/10.1175/2010jcl3611.1>

954 Fasullo, J., & Webster, P. J. (2003). A hydrological definition of Indian Monsoon onset and withdrawal.  
955 *Journal of Climate*, 16(19), 3200–3211. [https://doi.org/10.1175/1520-0442\(2003\)016<3200a:AHDOIM>2.0.CO;2](https://doi.org/10.1175/1520-0442(2003)016<3200a:AHDOIM>2.0.CO;2)

956 Fosu, B. O., & Wang, S. Y. S. (2015). Bay of Bengal: coupling of pre-monsoon tropical cyclones with  
957 the monsoon onset in Myanmar. *Climate Dynamics*, 45(3–4), 697–709.  
958 <https://doi.org/10.1007/s00382-014-2289-z>

959 Ghosh, S., Luniya, V., & Gupta, A. (2009). Trend analysis of Indian summer monsoon rainfall at  
960 different spatial scales. *Atmospheric Science Letters*, 10(4), 285–290.  
961 <https://doi.org/10.1002/ASL.235>

962 Gill, A. E. (1980). Some simple solutions for heat-induced tropical circulation. *Quarterly Journal of*  
963 *the Royal Meteorological Society*, 106(449), 447–462. <https://doi.org/10.1002/QJ.49710644905>

964 Goswami, B. N., Krishnamurthy, V., & Annmalai, H. (1999). A broad-scale circulation index for the

967 interannual variability of the Indian summer monsoon. *Quarterly Journal of the Royal*  
968 *Meteorological Society*, 125(554), 611–633. <https://doi.org/10.1002/qj.49712555412>

969 Goswami, B. N., & Xavier, P. K. (2005). ENSO control on the south Asian monsoon through the  
970 length of the rainy season. *Geophys Res Lett*, 32(18), L18717.  
971 <https://doi.org/10.1029/2005gl023216>

972 Hannachi, A. (2004). A primer for EOF analysis of climate data. *Reading: University of Reading*, 1–  
973 33. <http://www.o3d.org/eas-6490/lectures/EOFs/eofprimer.pdf>

974 Hersbach, H., Bell, B., Berrisford, P., Hirahara, S., Horányi, A., Muñoz-Sabater, J., Nicolas, J., Peubey,  
975 C., Radu, R., Schepers, D., Simmons, A., Soci, C., Abdalla, S., Abellán, X., Balsamo, G.,  
976 Bechtold, P., Biavati, G., Bidlot, J., Bonavita, M., ... Thépaut, J. N. (2020). The ERA5 global  
977 reanalysis. *Quarterly Journal of the Royal Meteorological Society*, 146(730), 1999–2049.  
978 <https://doi.org/10.1002/QJ.3803>

979 Htway, O., & Matsumoto, J. (2011). Climatological onset dates of summer monsoon over Myanmar.  
980 *International Journal of Climatology*, 31(3), 382–393. <https://doi.org/10.1002/JOC.2076>

981 Hu, P., Chen, S., Chen, W., & Tan, B. (2025). Asian–Pacific Summer Monsoon Variability and  
982 Atmospheric Teleconnection Patterns: Review and Outlook. *Journal of Meteorological Research*,  
983 39(3), 651–672. <https://doi.org/10.1007/s13351-025-4222-2>

984 Hu, P., Chen, W., Chen, S., & Huang, R. (2019). Interannual variability and triggers of the South China  
985 Sea summer monsoon withdrawal. *Climate Dynamics*, 53(7–8), 4355–4372.  
986 <https://doi.org/10.1007/s00382-019-04790-5>

987 Hu, P., Chen, W., Chen, S., Liu, Y., & Huang, R. (2020). Extremely Early Summer Monsoon Onset  
988 in the South China Sea in 2019 Following an El Niño Event. *Monthly Weather Review*, 148(5),  
989 1877–1890. <https://doi.org/10.1175/MWR-D-19-0317.1>

990 Hu, P., Chen, W., Wang, L., Chen, S., Liu, Y., & Chen, L. (2022). Revisiting the ENSO–monsoonal  
991 rainfall relationship: new insights based on an objective determination of the Asian summer  
992 monsoon duration. *Environmental Research Letters*, 17(10). <https://doi.org/10.1088/1748-9326/ac97ad>

993 Huang, S., Wang, B., & Wen, Z. (2020). Dramatic weakening of the tropical easterly jet projected by  
994 CMIP6 models. *Journal of Climate*, 33(19), 8439–8455. <https://doi.org/10.1175/JCLI-D-19-1002.1>

995 Jia, X., Yang, S., Li, X., Liu, Y., Wang, H., Liu, X., & Weaver, S. (2013). Prediction of global patterns  
996 of dominant quasi-biweekly oscillation by the NCEP Climate Forecast System version 2. *Climate*  
997 *Dynamics*, 41(5–6), 1635–1650. <https://doi.org/10.1007/S00382-013-1877-7>

1000 Jiao, D., Xu, N., Yang, F., & Xu, K. (2021). Evaluation of spatial-temporal variation performance of  
1001 ERA5 precipitation data in China. *Scientific Reports*, 11(1), 1–13.  
1002 <https://doi.org/10.1038/s41598-021-97432-y>

1003 K Lau, K. K. S. Y. (2000). Dynamical and boundary forcing characteristics of regional components of  
1004 the Asian summer monsoon. *J Clim*, 13, 2461–2482. [https://doi.org/10.1175/1520-0442\(2000\)013<2461:dabfco>2.0.co](https://doi.org/10.1175/1520-0442(2000)013<2461:dabfco>2.0.co)

1005 Kanamitsu, M., Ebisuzaki, W., Woollen, J., Yang, S. K., Hnilo, J. J., Fiorino, M., & Potter, G. L.  
1006 (2002). NCEP–DOE AMIP-II reanalysis (R-2). *Bulletin of the American Meteorological Society*,  
1007 83(11). <https://doi.org/10.1175/BAMS-83-11-1631>

1008 Kotal, S. D., Bhattacharya, S. K., Roy Bhowmik, S. K., & Kundu, P. K. (2014). Growth of cyclone  
1009 Viyaru and Phailin—A comparative study. *J. Earth Syst. Sci.*, 123(7), 1619–1635.

1010

1011 https://doi.org/10.1007/s12040-014-0493-1

1012 Krishnamurthy, V., & Kirtman, B. P. (2009). Relation between Indian monsoon variability and SST.  
1013 *Journal of Climate*, 22(17), 4437–4458. https://doi.org/10.1175/2009JCLI2520.1

1014 Krugman, P. R., Obstfeld, M., & Melitz, M. J. T. A.-T. T.-. (2018). *International economics : theory*  
1015 & policy (Eleventh e). Pearson New York. https://doi.org/LK  
1016 https://worldcat.org/title/1014329502

1017 Li, H., Dai, A., Zhou, T., & Lu, J. (2010). Responses of East Asian summer monsoon to historical SST  
1018 and atmospheric forcing during 1950–2000. *Climate Dynamics*, 34(4), 501–514.  
1019 https://doi.org/10.1007/S00382-008-0482-7

1020 Liu, Y., Cook, K. H., & Vizy, E. K. (2021). Delayed retreat of the summer monsoon over the Indochina  
1021 Peninsula linked to surface warming trends. *International Journal of Climatology*, 41(3), 1927–  
1022 1938. https://doi.org/10.1002/JOC.6938

1023 Loikith, P. C., Pampuch, L. A., Slinskey, E., Detzer, J., Mechoso, C. R., & Barkhordarian, A. (2019).  
1024 A climatology of daily synoptic circulation patterns and associated surface meteorology over  
1025 southern South America. *Climate Dynamics*, 53(7–8), 4019–4035.  
1026 https://doi.org/10.1007/S00382-019-04768-3/FIGURES/12

1027 Ma, Y. Z. (2019). Quantitative Geosciences: Data Analytics, Geostatistics, Reservoir Characterization  
1028 and Modeling. In *Quantitative Geosciences: Data Analytics, Geostatistics, Reservoir*  
1029 *Characterization and Modeling*. https://doi.org/10.1007/978-3-030-17860-4

1030 Mao, J., & Wu, G. (2007). Interannual variability in the onset of the summer monsoon over the Eastern  
1031 Bay of Bengal. *Theoretical and Applied Climatology*, 89(3–4), 155–170.  
1032 https://doi.org/10.1007/S00704-006-0265-1

1033 Oo, K. T. (2021). How El-Nino / La-Nina & India Ocean Dipole ( IDO ) Influence on Myanmar  
1034 Rainfall Distribution ( Statistical Analysis Report ) ( 1990-2019 ). *J Environ Sci. 2021*, 17(1),  
1035 178. https://doi.org/10.37532/environmental-science.2021.17.178

1036 Oo, K. T. (2022a). Interannual Variability of Winter Rainfall in Upper Myanmar. *Journal of*  
1037 *Sustainability and Environmental Management*, 1(3), 344–358.  
1038 https://doi.org/10.3126/josem.v1i3.48001

1039 Oo, K. T. (2022b). Interannual Variability of Winter Rainfall in Upper Myanmar. *Journal of*  
1040 *Sustainability and Environmental Management*, 1(3), 344–358.  
1041 https://doi.org/10.3126/JOSEM.V1I3.48001

1042 Oo, K. T. (2022c). Interannual Variability of Winter Rainfall in Upper Myanmar. *Journal of*  
1043 *Sustainability and Environmental Management*, 1(3), 344–358.  
1044 https://doi.org/https://doi.org/10.3126/josem.v1i3.48001

1045 Oo, K. T. (2023a). Climatology Definition of the Myanmar Southwest Monsoon (MSwM): Change  
1046 Point Index (CPI). *Advances in Meteorology*, 2023, 2346975.  
1047 https://doi.org/10.1155/2023/2346975

1048 Oo, K. T. (2023b). Climatology Definition of the Myanmar Southwest Monsoon (MSwM): Change  
1049 Point Index (CPI). *Advances in Meteorology*, 2023, 2346975.  
1050 https://doi.org/10.1155/2023/2346975

1051 Oo, K. T., Chen, H., Dong, Y., & Jonah, K. (2024). Investigating the link between Mainland-Indochina  
1052 monsoon onset dates and cyclones over the Bay of Bengal basin. *Climate Dynamics*.  
1053 https://doi.org/10.1007/S00382-024-07342-8

1054 Oo, K. T., Dalhatu, A., Jonah, K., Dong, Y., & Madhushanka, D. (2025). Examining of interannual  
1055 variability in the Mainland - Indochina Southwest Monsoon onset applying new monsoon index.  
1056 *Theoretical and Applied Climatology*. <https://doi.org/10.1007/s00704-025-05543-7>

1057 Oo, K. T., & Jonah, K. (2024). Interannual variation of summer southwest monsoon rainfall over the  
1058 monsoon core regions of the eastern Bay of Bengal and its relationship with oceans. *Journal of*  
1059 *Atmospheric and Solar-Terrestrial Physics*, 265, 106341.  
1060 <https://doi.org/10.1016/J.JASTP.2024.106341>

1061 Q Guo, J. W. (1988). A comparison of the summer precipitation in India with that in China. *J Trop*  
1062 *Meteorol*, 4, 53–60.

1063 Ramage, C. S. (1971). *Monsoon meteorology*. Academic Press.

1064 Ren, Q., Liu, F., Wang, B., Yang, S., Wang, H., & Dong, W. (2022). Origins of the Intraseasonal  
1065 Variability of East Asian Summer Precipitation. *Geophysical Research Letters*, 49(4).  
1066 <https://doi.org/10.1029/2021GL096574>

1067 Roxy, M. K., Dasgupta, P., McPhaden, M. J., Suematsu, T., Zhang, C., & Kim, D. (2019). Twofold  
1068 expansion of the Indo-Pacific warm pool warps the MJO life cycle. *Nature*, 575(7784), 647–651.  
1069 <https://doi.org/10.1038/s41586-019-1764-4>

1070 Roxy, M. K., Ritika, K., Terray, P., & Masson, S. (2014). The curious case of Indian Ocean warming.  
1071 *Journal of Climate*, 27(22), 8501–8509. <https://doi.org/10.1175/JCLI-D-14-00471.1>

1072 Sabeerali, C. T., Rao, S. A., George, G., Nagarjuna Rao, D., Mahapatra, S., Kulkarni, A., &  
1073 Murtugudde, R. (2014). Modulation of monsoon intraseasonal oscillations in the recent warming  
1074 period. *Journal of Geophysical Research*, 119(9), 5185–5203.  
1075 <https://doi.org/10.1002/2013JD021261>

1076 Salinger, M. J., Shrestha, M. L., Ailikun, Dong, W., McGregor, J. L., & Wang, S. (2014). Climate in  
1077 Asia and the Pacific: Climate Variability and Change. *Advances in Global Change Research*, 56,  
1078 17–57. [https://doi.org/10.1007/978-94-007-7338-7\\_2](https://doi.org/10.1007/978-94-007-7338-7_2)

1079 Sawyer, J. S. (1947). The structure of the intertropical front over N.W. India during the S.W. Monsoon.  
1080 *Quarterly Journal of the Royal Meteorological Society*, 73(317–318), 346–369.  
1081 <https://doi.org/10.1002/QJ.49707331709>

1082 Schmidhammer. (2000). Box Plot and Robust Statistics. *Matrix*, 5, 109–122.

1083 Seager, R., Naik, N., & Vecchi, G. A. (2010). Thermodynamic and dynamic mechanisms for large-  
1084 scale changes in the hydrological cycle in response to global warming. *Journal of Climate*, 23(17),  
1085 4651–4668. <https://doi.org/10.1175/2010JCLI3655.1>

1086 Selman, C., & Misra, V. (2014). The Met Office Hadley Centre sea ice and sea surface temperature  
1087 data set, version 2: 1. Sea ice concentrations. *Journal of Geophysical Research*, 3, 180–198.  
1088 <https://doi.org/10.1002/2013JD021040>. Received

1089 Sharmila, S., Pillai, P. A., Joseph, S., Roxy, M., Krishna, R. P. M., Chattopadhyay, R., Abhilash, S.,  
1090 Sahai, A. K., & Goswami, B. N. (2013). Role of ocean-atmosphere interaction on northward  
1091 propagation of Indian summer monsoon intra-seasonal oscillations (MISO). *Climate Dynamics*,  
1092 41(5–6), 1651–1669. <https://doi.org/10.1007/S00382-013-1854-1>

1093 Song, L., Hu, P., Chen, W., Yang, R., Ma, T., & Zheng, Y. (2025). Increasing Trend of Summer  
1094 Monsoonal Rainfall Tied to the Extension of the South China Sea Summer Monsoon Duration.  
1095 *Atmospheric Science Letters*, 26(7), 1–9. <https://doi.org/10.1002/asl.1308>

1096 Sreekala, P. P., Bhaskara Rao, S. V., Arunachalam, M. S., & Harikiran, C. (2014). A study on the

1097 decreasing trend in tropical easterly jet stream (TEJ) and its impact on Indian summer monsoon  
1098 rainfall. *Theoretical and Applied Climatology*, 118(1–2), 107–114.  
1099 <https://doi.org/10.1007/s00704-013-1049-z>

1100 Than Oo, K., Datti, A. D., Jonah, K., & Ayugi, B. O. (2025). The Complex Teleconnections and  
1101 Feedback Mechanisms between Mainland Indochina's Southwest Monsoon and Arctic Ocean  
1102 Climate Variability. *EGUspHERE*, 2025, 1–32. <https://doi.org/10.5194/egusphere-2025-521>

1103 Vijaya Kumari, K., Karuna Sagar, S., Viswanadhapalli, Y., Dasari, H. P., & Bhaskara Rao, S. V. (2018).  
1104 Role of planetary boundary layer processes on the simulation of tropical cyclones over Bay of  
1105 Bengal. *Pure and Applied Geophysics*, 176(2), 951–977. <https://doi.org/10.1007/s00024-018-2017-4>

1107 Walker, J. M., Bordoni, S., & Schneider, T. (2015). Interannual variability in the large-scale dynamics  
1108 of the South Asian summer monsoon. *Journal of Climate*, 28(9), 3731–3750.  
1109 <https://doi.org/10.1175/JCLI-D-14-00612.1>

1110 Wang, B., & Ho, L. (2002). Rainy season of the Asian-Pacific summer monsoon. *Journal of Climate*,  
1111 15(4), 386–398. [https://doi.org/10.1175/1520-0442\(2002\)015<0386:RSOTAP>2.0.CO;2](https://doi.org/10.1175/1520-0442(2002)015<0386:RSOTAP>2.0.CO;2)

1112 Wang, B., Huang, F., Wu, Z., Yang, J., Fu, X., & Kikuchi, K. (2009). Multi-scale climate variability  
1113 of the South China Sea monsoon: A review. *Dynamics of Atmospheres and Oceans*, 47(1), 15–  
1114 37. <https://doi.org/https://doi.org/10.1016/j.dynatmoce.2008.09.004>

1115 Wang, B., LinHo, Zhang, Y., & Lu, M. M. (2004). Definition of South China Sea monsoon onset and  
1116 commencement of the East Asian summer monsoon. *Journal of Climate*, 17(4), 699–710.  
1117 <https://doi.org/10.1175/2932.1>

1118 Wang, B., Wu, R., & Lau, K. M. (2001). Interannual variability of the asian summer monsoon:  
1119 Contrasts between the Indian and the Western North Pacific-East Asian monsoons. *Journal of  
1120 Climate*, 14(20), 4073–4090. [https://doi.org/10.1175/1520-0442\(2001\)014<4073:IVOTAS>2.0.CO;2](https://doi.org/10.1175/1520-0442(2001)014<4073:IVOTAS>2.0.CO;2)

1122 Wang, B., Wu, Z., Li, J., Liu, J., Chang, C. P., Ding, Y., & Wu, G. (2008). How to measure the strength  
1123 of the East Asian summer monsoon. *Journal of Climate*, 21(17), 4449–4463.  
1124 <https://doi.org/10.1175/2008JCLI2183.1>

1125 Wang, X., & Zhou, W. (2024). Interdecadal variation of the monsoon trough and its relationship with  
1126 tropical cyclone genesis over the South China Sea and Philippine Sea around the mid-2000s.  
1127 *Climate Dynamics*, 62(5), 3743–3762. <https://doi.org/10.1007/s00382-023-07096-9>

1128 Webster, P. J., & Yang, S. (1992). Monsoon and Enso: Selectively Interactive Systems. *Quarterly  
1129 Journal of the Royal Meteorological Society*, 118(507), 877–926.  
1130 <https://doi.org/10.1002/qj.49711850705>

1131 Win Zin, W., & Rutten, M. (2017). Long-term Changes in Annual Precipitation and Monsoon Seasonal  
1132 Characteristics in Myanmar. *Hydrology: Current Research*, 08(02). <https://doi.org/10.4172/2157-7587.1000271>

1134 Wu, R. (2017). Relationship between Indian and East Asian summer rainfall variations. *Advances in  
1135 Atmospheric Sciences*, 34(1), 4–15. <https://doi.org/10.1007/S00376-016-6216-6>

1136 Wu, X., & Mao, J. (2018). Spatial and interannual variations of spring rainfall over eastern China in  
1137 association with PDO–ENSO events. *Theoretical and Applied Climatology*, 134(3–4), 935–953.  
1138 <https://doi.org/10.1007/s00704-017-2323-2>

1139 Xing, N., Li, J., & Wang, L. (2016). Effect of the early and late onset of summer monsoon over the  
1140 Bay of Bengal on Asian precipitation in May. *Climate Dynamics*, 47(5–6), 1961–1970.

1141 https://doi.org/10.1007/s00382-015-2944-z

1142 Xu, C., Wang, S. Y. S., Borhara, K., Buckley, B., Tan, N., Zhao, Y., An, W., Sano, M., Nakatsuka, T.,  
1143 & Guo, Z. (2023). Asian-Australian summer monsoons linkage to ENSO strengthened by global  
1144 warming. *Npj Climate and Atmospheric Science*, 6(1). <https://doi.org/10.1038/S41612-023-00341-2>

1145

1146 Zhang, H., Liang, P., Moise, A., & Hanson, L. (2012). Diagnosing potential changes in Asian summer  
1147 monsoon onset and duration in IPCC AR4 model simulations using moisture and wind indices.  
1148 *Climate Dynamics*, 39(9–10), 2465–2486. <https://doi.org/10.1007/s00382-012-1289-0>

1149 Zhang, S., Qu, X., Huang, G., Hu, P., Zhou, S., & Wu, L. (2024). Delayed Onset of Indian Summer  
1150 Monsoon in Response to CO<sub>2</sub> Removal. *Earth's Future*, 12(2), 1–17.  
1151 <https://doi.org/10.1029/2023EF004039>

1152 Zhang, Y., Li, T., Wang, B., & Wu, G. (2002a). Onset of the summer monsoon over the Indochina  
1153 Peninsula: Climatology and interannual variations. *Journal of Climate*, 15(22), 3206–3221.  
1154 [https://doi.org/10.1175/1520-0442\(2002\)015<3206:OOTSMO>2.0.CO;2](https://doi.org/10.1175/1520-0442(2002)015<3206:OOTSMO>2.0.CO;2)

1155 Zhang, Y., Li, T., Wang, B., & Wu, G. (2002b). Onset of the Summer Monsoon over the Indochina  
1156 Peninsula: Climatology and Interannual Variations. *Journal of Climate*, 15(22), 3206–3221.  
1157 [https://doi.org/10.1175/1520-0442\(2002\)015<3206:OOTSMO>2.0.CO;2](https://doi.org/10.1175/1520-0442(2002)015<3206:OOTSMO>2.0.CO;2)

1158 Zin Mie Mie Sein, B. Ogwang, V. Ongoma, Faustin Katchele Ogomou, & Kpaikpai Batebana. (2015).  
1159 *Inter-annual variability of Summer Monsoon Rainfall over Myanmar in relation to IOD and*  
1160 *ENSO* (pp. 4:28–36). Journal of Environmental and Agricultural Sciences.

1161

← **Formatted:** Indent: Left: 0", Hanging: 0.33", Don't  
adjust right indent when grid is defined, Line spacing:  
single, No widow/orphan control, Don't adjust space  
between Latin and Asian text, Don't adjust space  
between Asian text and numbers